Stress equilibrium in southern California from Maxwell stress function models fit to both earthquake data and a quasi-static dynamic simulation

Peter Bird
Dept. of Earth, Planetary, and Space Sciences
UCLA
for the CSM Workshop 2014.10.27 in Pomona, CA

SCEC
an NSF+USGS center

Assumptions & Approximations

- Flat-Earth approximation (Cartesian coordinates), with preferred map-projection used to translate (*lon, lat*) to (*x, y*).
- Model volume is a rectangular solid with sides of 750 × 600 × 75~100 km (= SCEC area x lithosphere thickness, + top of asthenosphere).

Digital Elevation Model
& Location of sections A, B, C

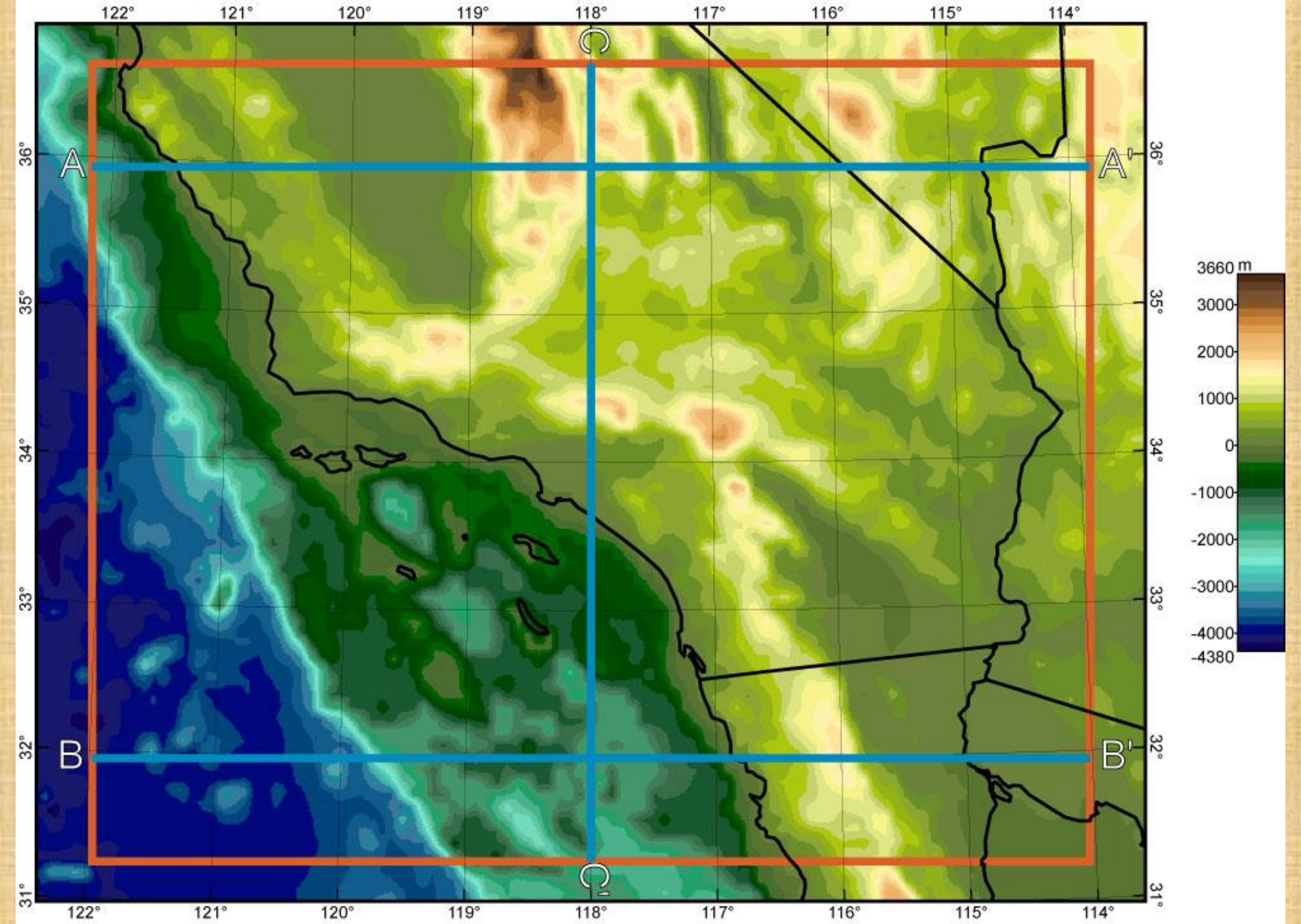

Assumptions & Approximations

- Flat-Earth approximation (Cartesian coordinates), with preferred map-projection used to translate (*lon, lat*) to (*x, y*).
- Model volume is a rectangular solid with sides of 750 × 600 × 75~100 km (= SCEC area x lithosphere thickness, + top of asthenosphere).
- Gravity is the only body force, and is exactly parallel to *z*.
- Quasi-static equilibrium between earthquakes, eruptions, impacts, landslides, *etc.*

In this Cartesian model space, the quasi-static momentum equation (or stress-equilibrium equation) is

$$
\begin{cases}
\dfrac{\partial \sigma_{xx}}{\partial x} + \dfrac{\partial \sigma_{xy}}{\partial y} + \dfrac{\partial \sigma_{xz}}{\partial z} = 0 \\[2ex]
\dfrac{\partial \sigma_{yx}}{\partial x} + \dfrac{\partial \sigma_{yy}}{\partial y} + \dfrac{\partial \sigma_{yz}}{\partial z} = 0 \\[2ex]
\dfrac{\partial \sigma_{zx}}{\partial x} + \dfrac{\partial \sigma_{zy}}{\partial y} + \dfrac{\partial \sigma_{zz}}{\partial z} = \rho g
\end{cases}
$$

In terms of the stress tensor $\tilde{\sigma}$, gravity $\vec{g}$, and density ρ.

Next, stress $\tilde{\sigma}$ is expressed as a sum of 3 components:

$$\tilde{\sigma} \equiv -P_0(z)\tilde{I} + \tilde{\mu} + \tilde{\tau}$$

where $P_0 \equiv g\int_z^\infty \rho_0(s)\,\mathrm{d}s$ is a ***reference lithostatic pressure curve***,

based on a 1-D reference density model $\rho_0(\mathrm{z})$,

$\tilde{\mu}$ is the ***topographic stress anomaly***,

and $\tilde{\tau}$ is the ***tectonic stress anomaly***.

Specifically, I define $\tilde{\mu}$ as any *convenient* solution to the

Inhomogeneous quasi-static momentum equation driven by density anomaly

$\Delta\rho(x,y,z) \equiv \rho(x,y,z) - \rho_0(z)$:

$$\begin{cases} \dfrac{\partial \mu_{xx}}{\partial x} + \dfrac{\partial \mu_{xy}}{\partial y} + \dfrac{\partial \mu_{xz}}{\partial z} = 0 \\ \dfrac{\partial \mu_{yx}}{\partial x} + \dfrac{\partial \mu_{yy}}{\partial y} + \dfrac{\partial \mu_{yz}}{\partial z} = 0 \\ \dfrac{\partial \mu_{zx}}{\partial x} + \dfrac{\partial \mu_{zy}}{\partial y} + \dfrac{\partial \mu_{zz}}{\partial z} = \Delta\rho g \end{cases}$$

and $\tilde{\tau}$ as any solution to the complementary homogeneous quasi-static momentum equation:

$$
\begin{cases}
\dfrac{\partial \tau_{xx}}{\partial x} + \dfrac{\partial \tau_{xy}}{\partial y} + \dfrac{\partial \tau_{xz}}{\partial z} = 0 \\
\dfrac{\partial \tau_{yx}}{\partial x} + \dfrac{\partial \tau_{yy}}{\partial y} + \dfrac{\partial \tau_{yz}}{\partial z} = 0 \\
\dfrac{\partial \tau_{zx}}{\partial x} + \dfrac{\partial \tau_{zy}}{\partial y} + \dfrac{\partial \tau_{zz}}{\partial z} = 0
\end{cases}
$$

The sum $\tilde{\mu} + \tilde{\tau}$ will be referred to as the "total stress anomaly" (relative to standardized reference pressure).

Note that total stress anomaly is *not the same* as deviatoric stress, although it shares the same principle axes as deviatoric stress.

The deviatoric stress matrix has zero trace, but the total stress anomaly matrix *does not*.

The most convenient solutions for the topographic stress anomaly come from classic published solutions for an isotropic and homogenous elastic half-space, with no density or pre-stress, but subject to:

- Vertical surface point loads (Boussinesq);
- Horizontal surface point loads (Cerruti); and
- Vertical internal point loads (Mindlin).

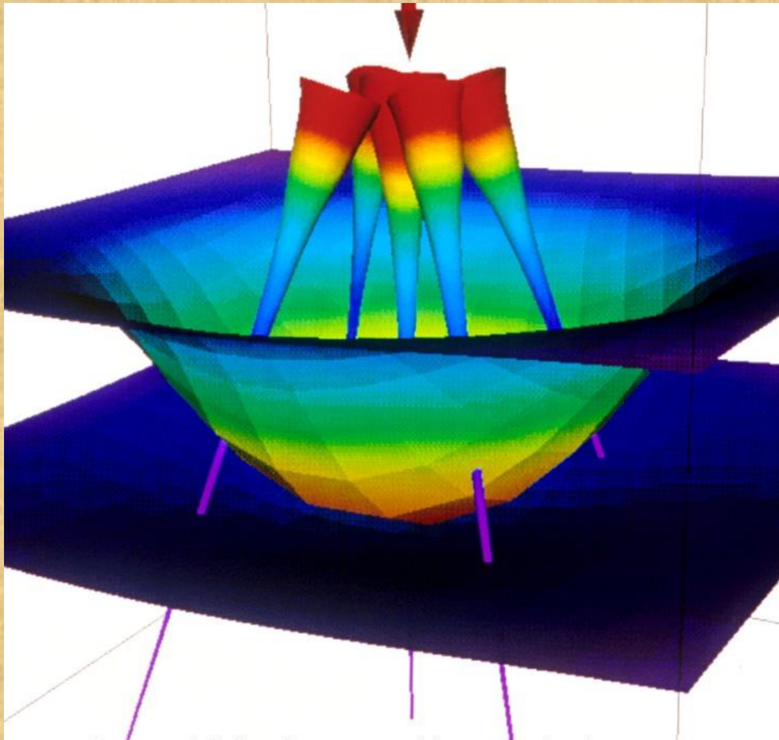
tractions and deflections caused by point load orthogonal to flat surface of elastic half-space

The only material property in these solutions is the Poisson ratio. One natural choice is 0.25, based on the common relation between compressional and shear seismic velocities that $V_S \cong V_P / \sqrt{3}$.

However, topographic (and tectonic) stress anomalies last for millions of years, during which there may be some viscoelastic relaxation. It is well-known that the long-term asymptotic stresses in *viscoelastic* solutions to problems with *traction* boundary conditions resemble *elastic* solutions with an incompressible Poisson ratio of 0.5, because viscous permanent strain mechanisms conserve volume.

Therefore, I computed topographic stress anomaly solutions with both values of the Poisson ratio.

In general, the solutions with Poisson ratio 0.25 have greater shear stresses and smaller pressure anomalies, while the solutions with Poisson ration 0.5 have smaller shear stresses and larger pressure anomalies.

Another choice is how to model the Moho shape.
I have tried models with seismic Moho shapes, and others with isostatic Moho shapes. I prefer the isostatic Moho models because they give less deviatoric stress in the upper asthenosphere.

Topographic stress anomaly model HiResIso0p50
Greatest shear stress in horizontal plane 10 km below MSL

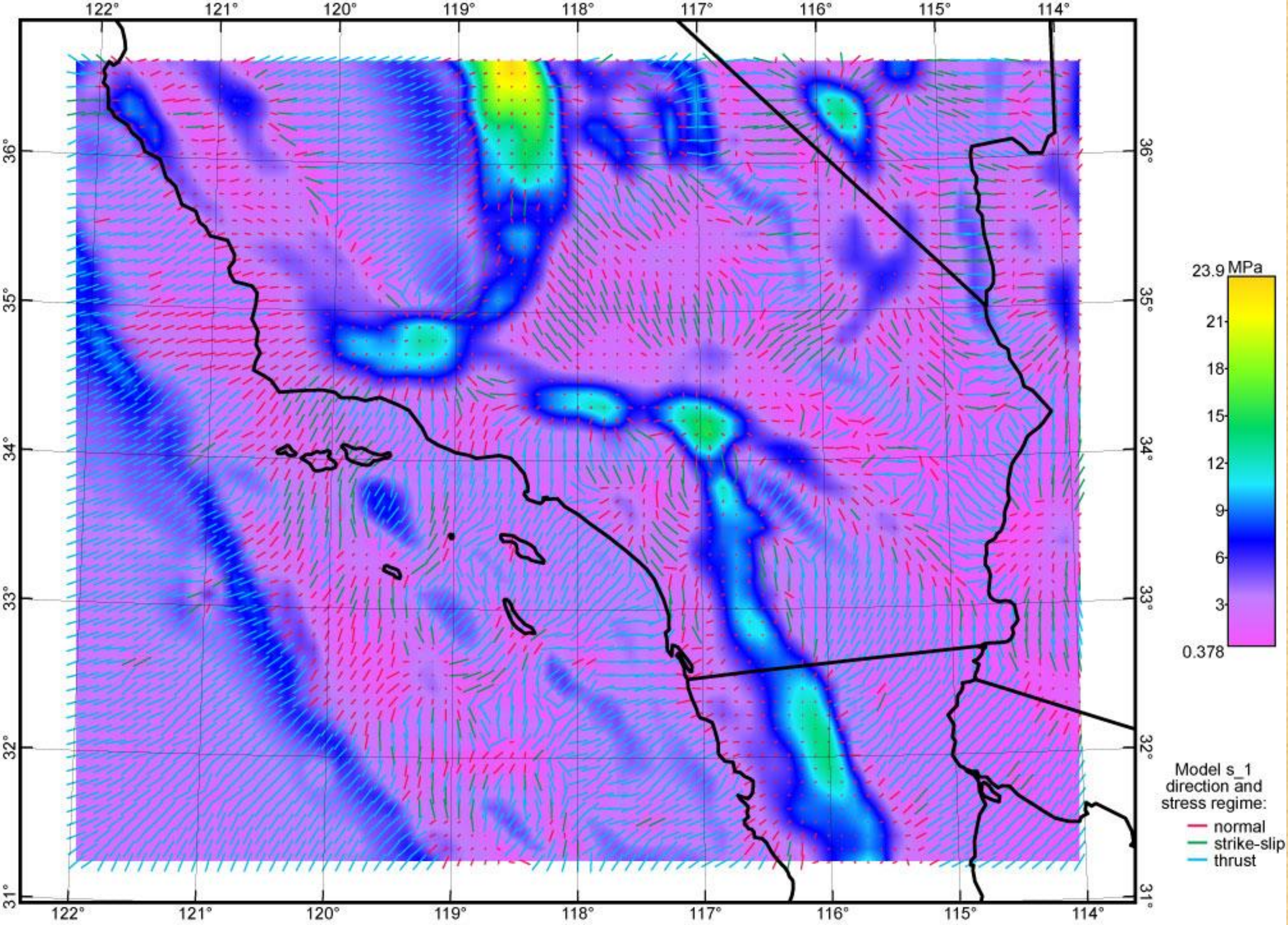

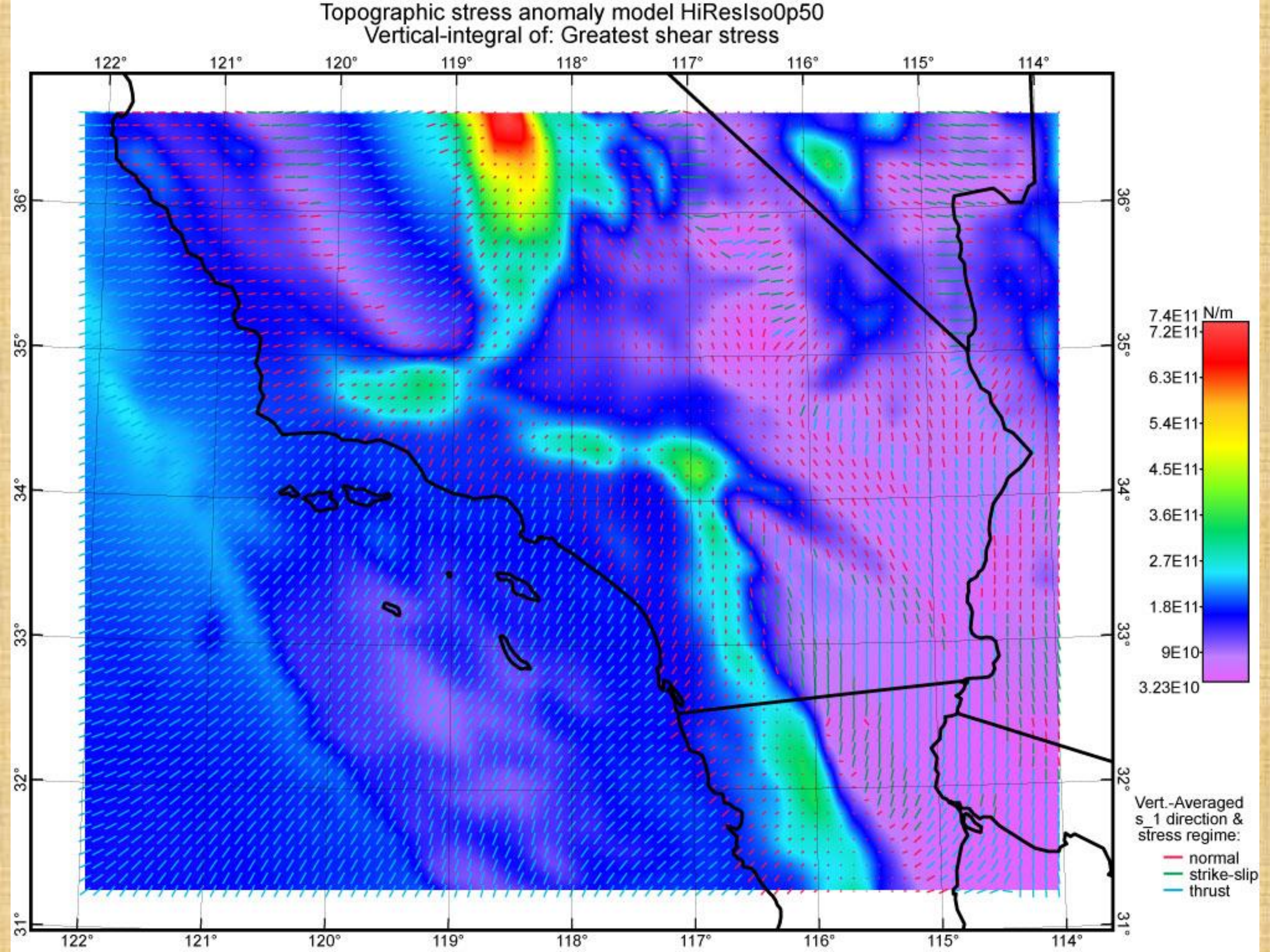

Topographic stress anomaly model HiResIso0p50
Vertical-integral of: Greatest shear stress
122°
121°
120°
119°
118°
117°
116°
115°
114°
36°
35°
34°
33°
32°
31°
N/m
7.4E11
7.2E11
6.3E11
5.4E11
4.5E11
3.6E11
2.7E11
1.8E11
9E10
3.23E10
Vert.-Averaged
s_1 direction &
stress regime:
normal
strike-slip
thrust

Topographic stress anomaly model HiResIso0p50
Pressure anomaly at plane of section

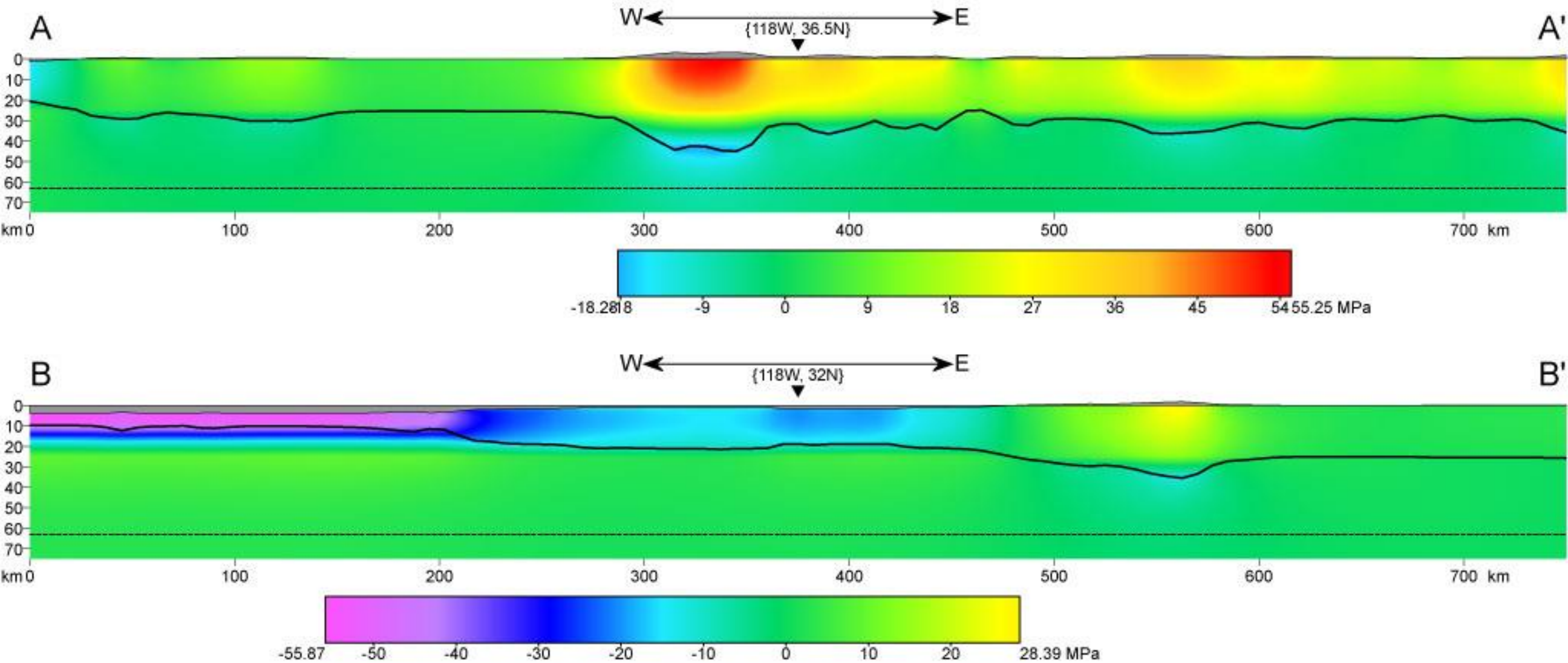

Topographic stress anomaly model HiResIso0p50
Greatest shear stress at plane of section

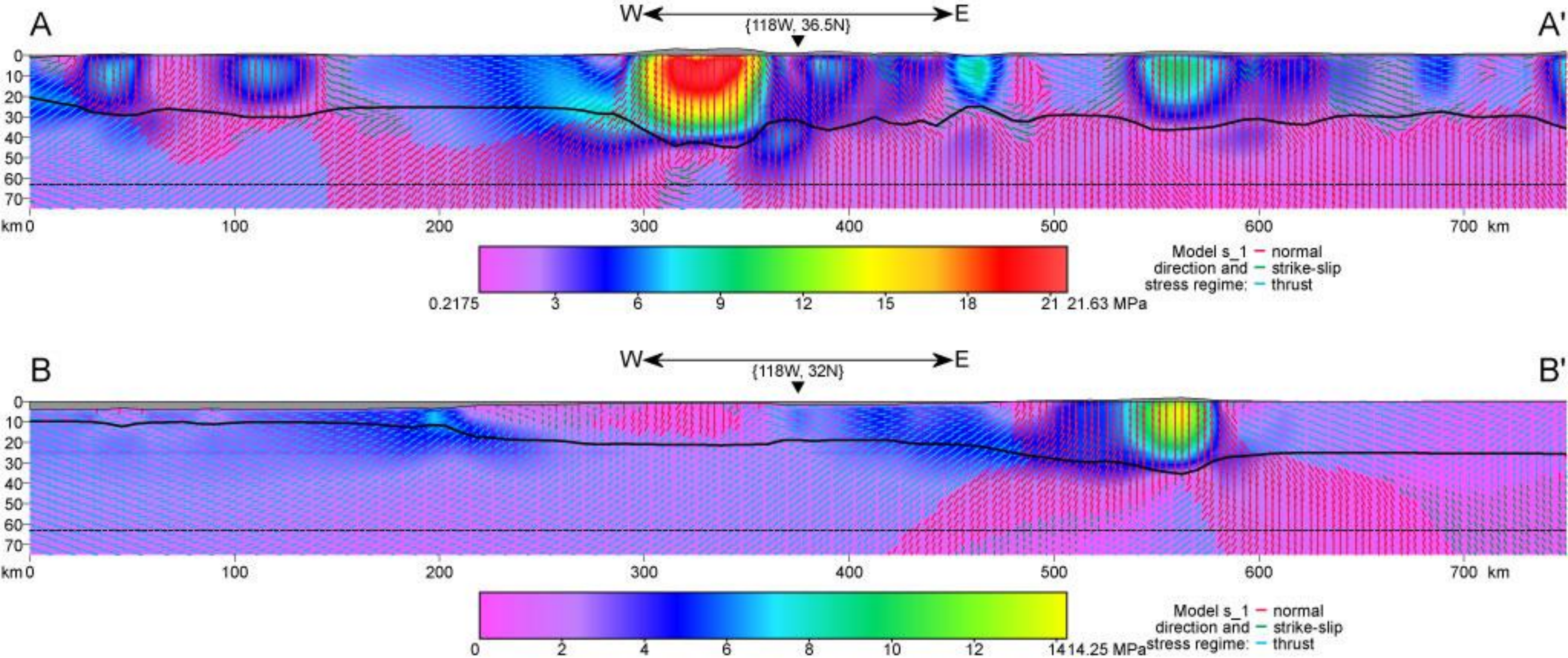

The tectonic stress anomaly $\tilde{\tau}$ satisfies the homogeneous quasi-static momentum equation, and therefore it can be obtained from particular second-derivatives of a continuous vector field $\vec{\Phi}$ by:

$$\begin{cases} \tau_{xx} = \dfrac{\partial^2 \Phi_z}{\partial y^2} + \dfrac{\partial^2 \Phi_y}{\partial z^2} \quad \tau_{yy} = \dfrac{\partial^2 \Phi_x}{\partial z^2} + \dfrac{\partial^2 \Phi_z}{\partial x^2} \quad \tau_{zz} = \dfrac{\partial^2 \Phi_y}{\partial x^2} + \dfrac{\partial^2 \Phi_x}{\partial y^2} \\ \tau_{xy} = \tau_{yx} = -\dfrac{\partial^2 \Phi_z}{\partial x \partial y} \quad \tau_{yz} = \tau_{zy} = -\dfrac{\partial^2 \Phi_x}{\partial y \partial z} \quad \tau_{xz} = \tau_{zx} = -\dfrac{\partial^2 \Phi_y}{\partial x \partial z} \end{cases}$$

This was apparently first discovered by William Thompson (later, Lord Kelvin) and published in Maxwell [1848].

Fig. 1. James Clerk Maxwell, 24 years old in 1855, about the time he embarked on unifying electrostatics, electrodynamics, and electrical induction. He was inspired by Faraday's intuition and by Fourier's mathematics of diffusion. (Photograph by W.H. Hales; courtesy of Cavendish Laboratories.)

Narasimhan [2003]

Although I have been unable to examine this original source, secondary sources include Love [1927], Sadd [2005], and the Wikipedia entry "Stress functions".

I explore possible vector fields $\vec{\Phi}$ which are formed as weighted sums of $i = 1, \ldots, N$ basis functions,

$$\vec{\Phi}(x, y, z) = \sum_{i=1}^{N} c_i \vec{\Phi}^i(x, y, z)$$

I have designed a complete and complementary set of basis functions which provide for:

(1) spatially-constant values of each tectonic stress component;
(2) values of any tectonic stress component that may vary linearly along any spatial axis;

(3) stress-potential vectors of arbitrary direction that vary harmonically as a function of any one space direction (“stress waves”);

(4) stress-potential vectors that vary harmonically as a function of any two space directions (“stress quilts”); and

(5) stress-potential vectors that vary harmonically as function of all three space directions (“stress crystals”).

Hybrid coefficient c_3,6,5,0
Pressure anomaly on horizontal plane 10 km below MSL

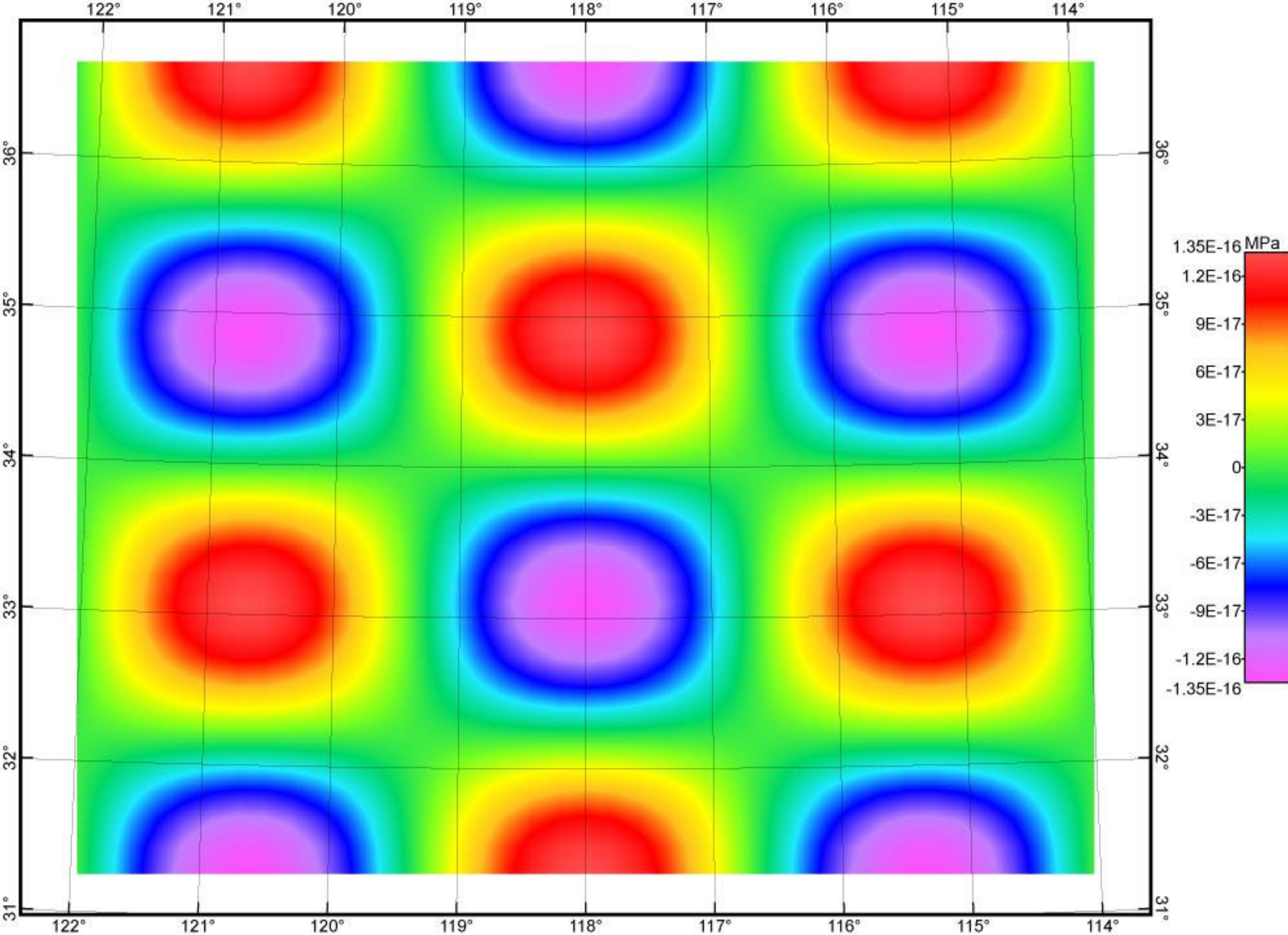

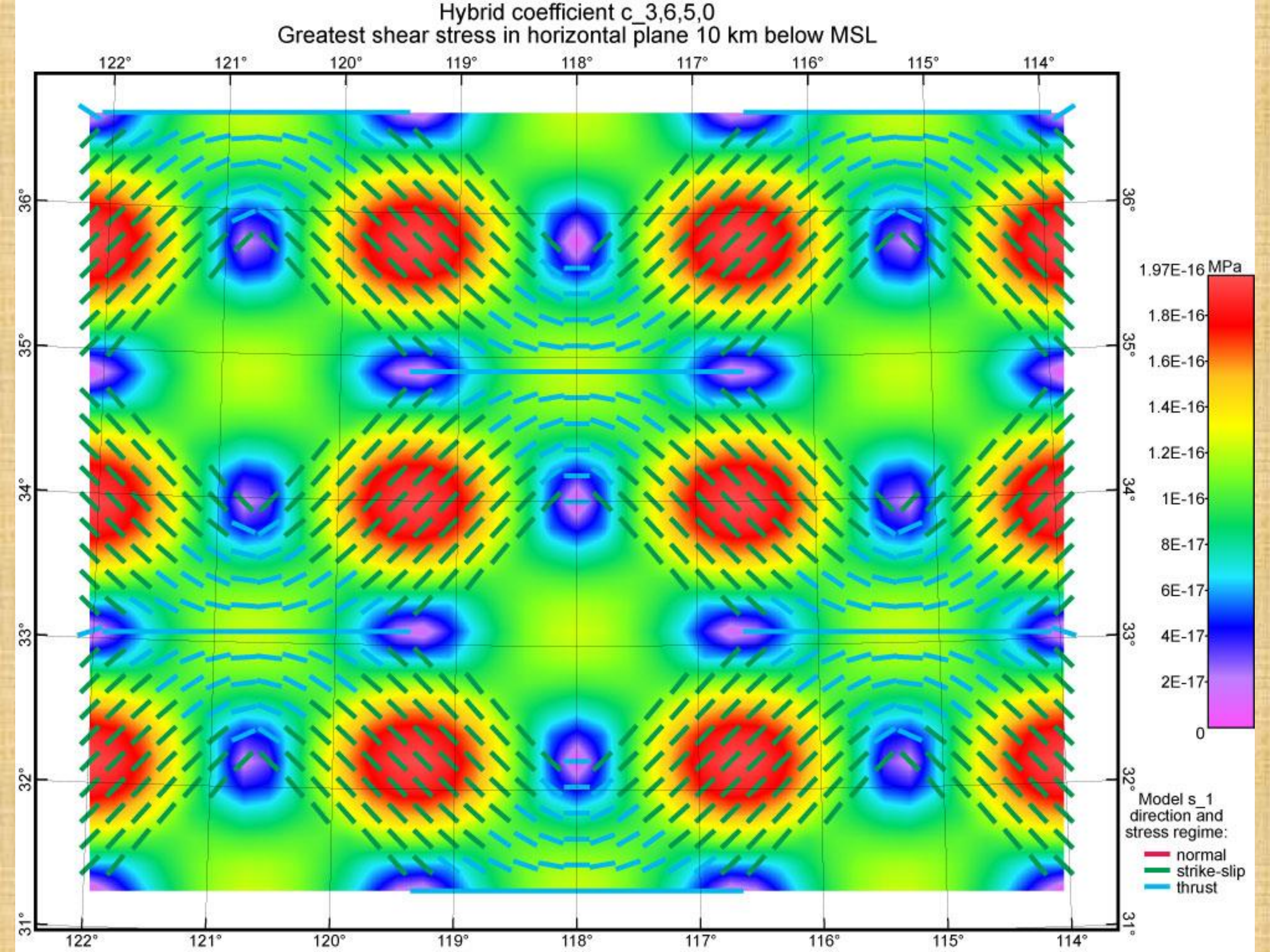
Hybrid coefficient c_3,6,5,0
Greatest shear stress in horizontal plane 10 km below MSL
122°
121°
120°
119°
118°
117°
116°
115°
114°
36°
35°
34°
33°
32°
31°
1.97E-16 MPa
1.8E-16
1.6E-16
1.4E-16
1.2E-16
1E-16
8E-17
6E-17
4E-17
2E-17
0
Model s_1 direction and stress regime:
normal
strike-slip
thrust

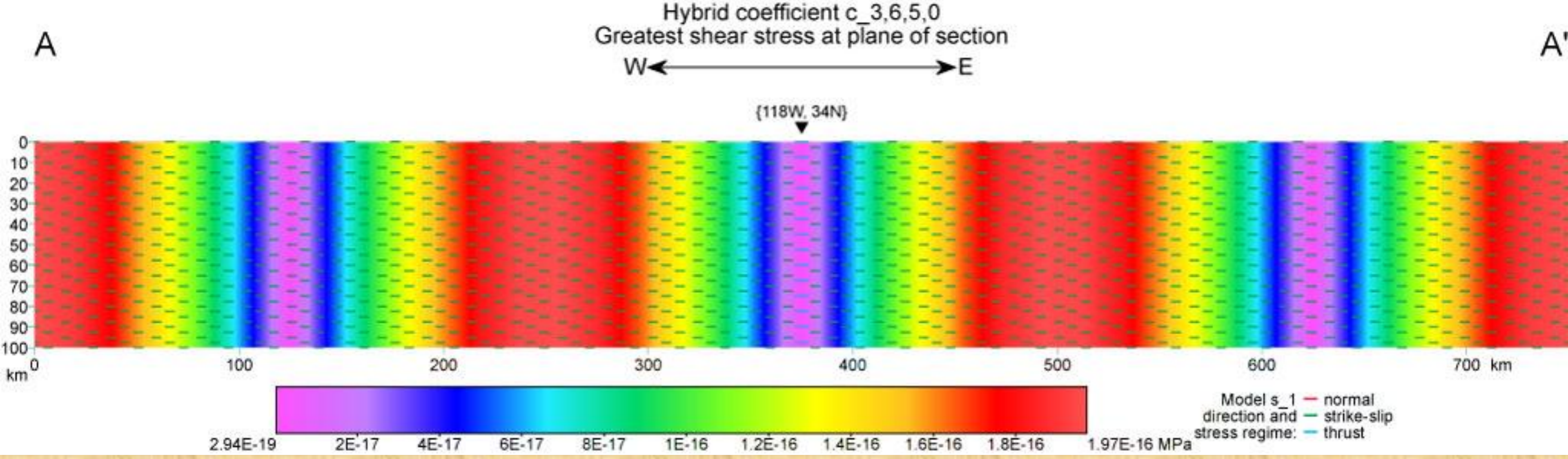
Hybrid coefficient c_3,6,5,0
Greatest shear stress at plane of section
A
A'
W
E
{118W, 34N}
0
10
20
30
40
50
60
70
80
90
100
km
0
100
200
300
400
500
600
700 km
2.94E-19
2E-17
4E-17
6E-17
8E-17
1E-16
1.2E-16
1.4E-16
1.6E-16
1.8E-16
1.97E-16 MPa
Model s_1 direction and stress regime:
normal
strike-slip
thrust

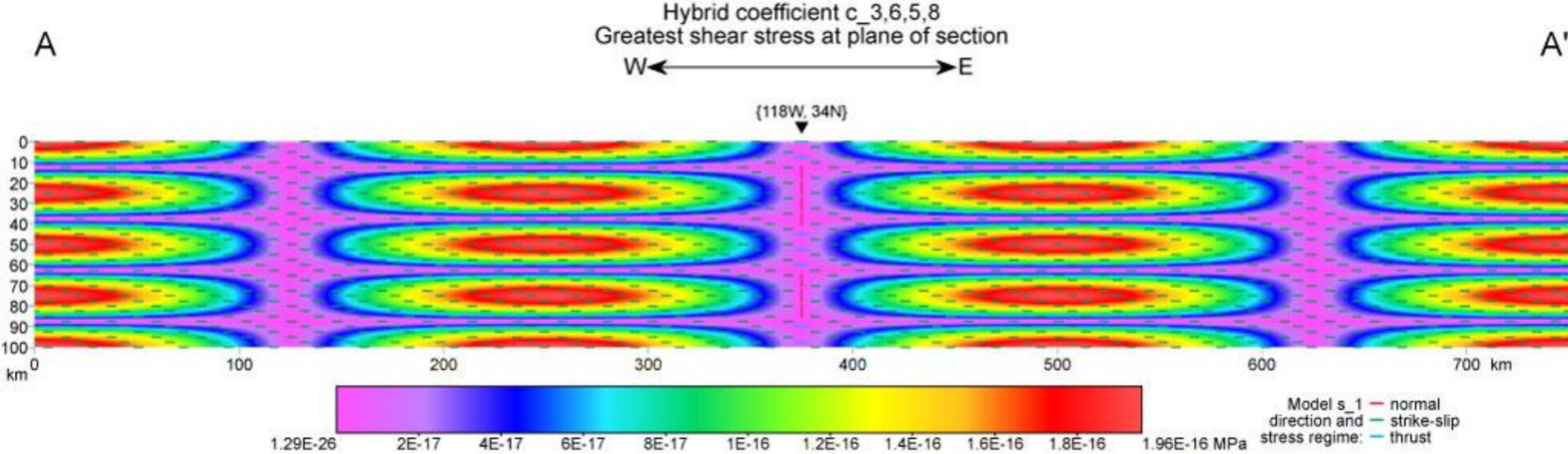
A
A'
Hybrid coefficient c_3,6,5,8
Greatest shear stress at plane of section
W
E
{118W, 34N}
0
10
20
30
40
50
60
70
80
90
100
km
0
100
200
300
400
500
600
700 km
1.29E-26
2E-17
4E-17
6E-17
8E-17
1E-16
1.2E-16
1.4E-16
1.6E-16
1.8E-16
1.96E-16 MPa
Model s_1 direction and stress regime:
normal
strike-slip
thrust

One way to approach a unique solution for $\vec{\Phi}$ and $\tilde{\tau}$ is to assume the material is elastic, and is also lacking any pre-stress.

This engineering approach is not suitable for Earth sciences, in which we have to expect a long history (with *unknown initial conditions*) involving complex combinations of elasticity with pressure changes, temperature changes, compaction, solution transfer, dislocation creep, metamorphic phase changes, cracking events, and frictional failures.

In this project I pursued another approach: fitting $\vec{\Phi}$ and $\tilde{\tau}$ to a combination of boundary conditions, data, and a dynamic model by weighted least-squares.

The soft constraints imposed in this study included:

(1) Boundary conditions: No tractions due to tectonic stress on the horizontal plane at sea level. No tractions due the total stress anomaly on the model base (and lower sides) in the asthenospheric depth range.

(2A) Stress data from the World Stress Map [*Heidbach et al.*, 2008]: 449 data, with only 9 constraints on stress magnitude; OR …

Most-compressive stress directions & regimes from World Stress Map 2008 dataset
wsm2008.csv (449 orientations in model box)

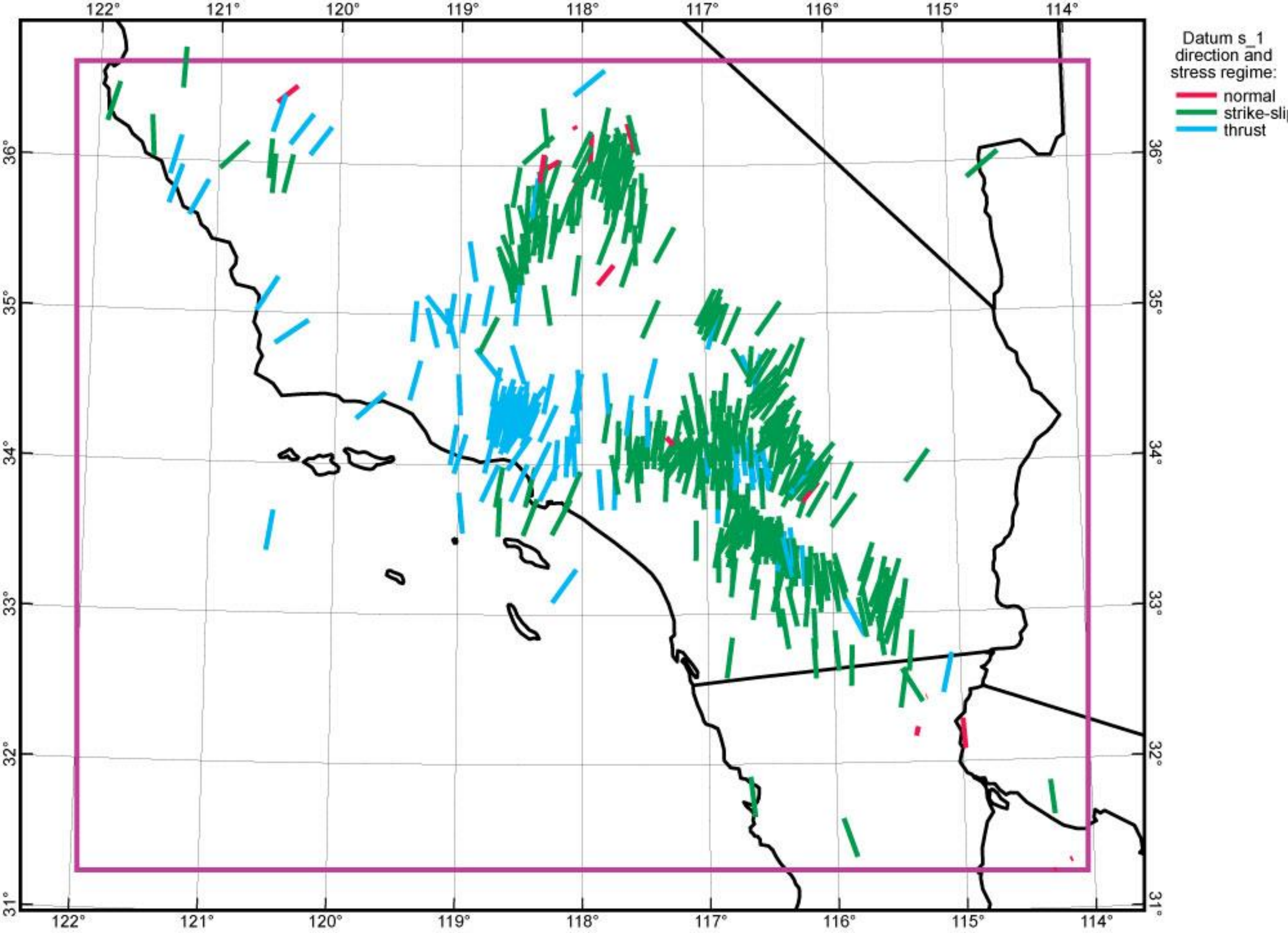

The soft constraints imposed in this study included:

(1) Boundary conditions: No tractions due to tectonic stress on the horizontal plane at sea level. No tractions due the total stress anomaly on the model base (and lower sides) in the asthenospheric depth range.

(2A) Stress data from the World Stress Map [*Heidbach et al.*, 2008]: 449 data, with only 9 constraints on stress magnitude; OR …

(2B) Stress directions from 178152 focal mechanisms of *Yang et al.* [2012, BSSA].

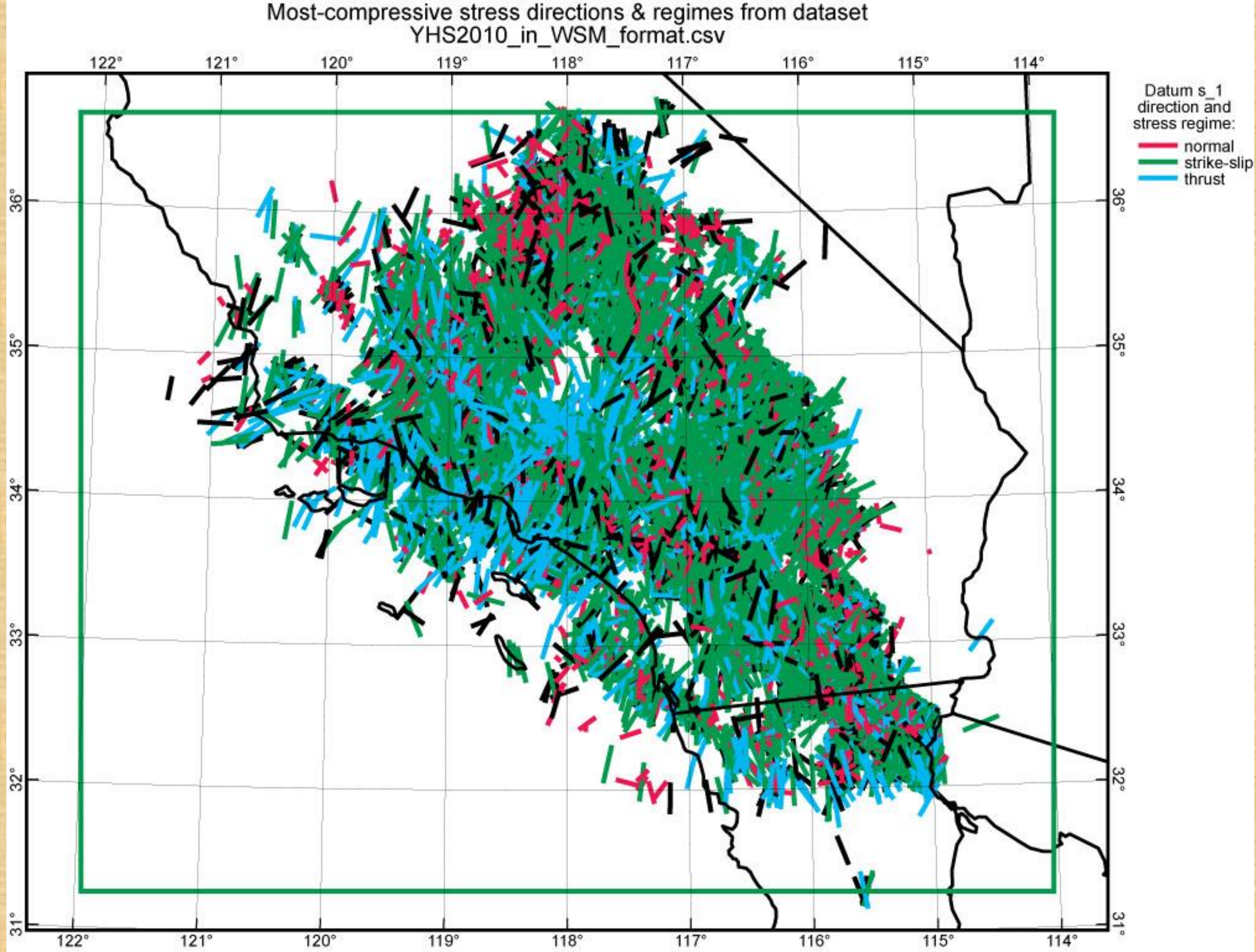
Most-compressive stress directions & regimes from dataset
YHS2010_in_WSM_format.csv
Datum s_1
direction and
stress regime:
normal
strike-slip
thrust
122°
121°
120°
119°
118°
117°
116°
115°
114°
36°
35°
34°
33°
32°
31°

The soft constraints imposed in this study included:

(1) Boundary conditions: No tractions due to tectonic stress on the horizontal plane at sea level. No tractions due the total stress anomaly on the model base (and lower sides) in the asthenospheric depth range.

(2A) Stress data from the World Stress Map [*Heidbach et al.*, 2008]: 449 data, with only 9 constraints on stress magnitude; OR …

(2B) Stress directions from 178152 focal mechanisms of *Yang et al.* [2012, BSSA].

(3) Stress directions and magnitudes in 3-D from a 2.5-D thin-shell model of southern California neotectonics computed with **Shells**, using variable heat-flow, crustal thickness, & lithosphere thickness; UCERF3 fault traces, and plate-tectonics (PA-NA) velocity boundary conditions.

Vertical Integrals of Shear Stress and Stress Anomaly
CSM2013001, using SHELLS_for_CSM-faulted_expanded.feg

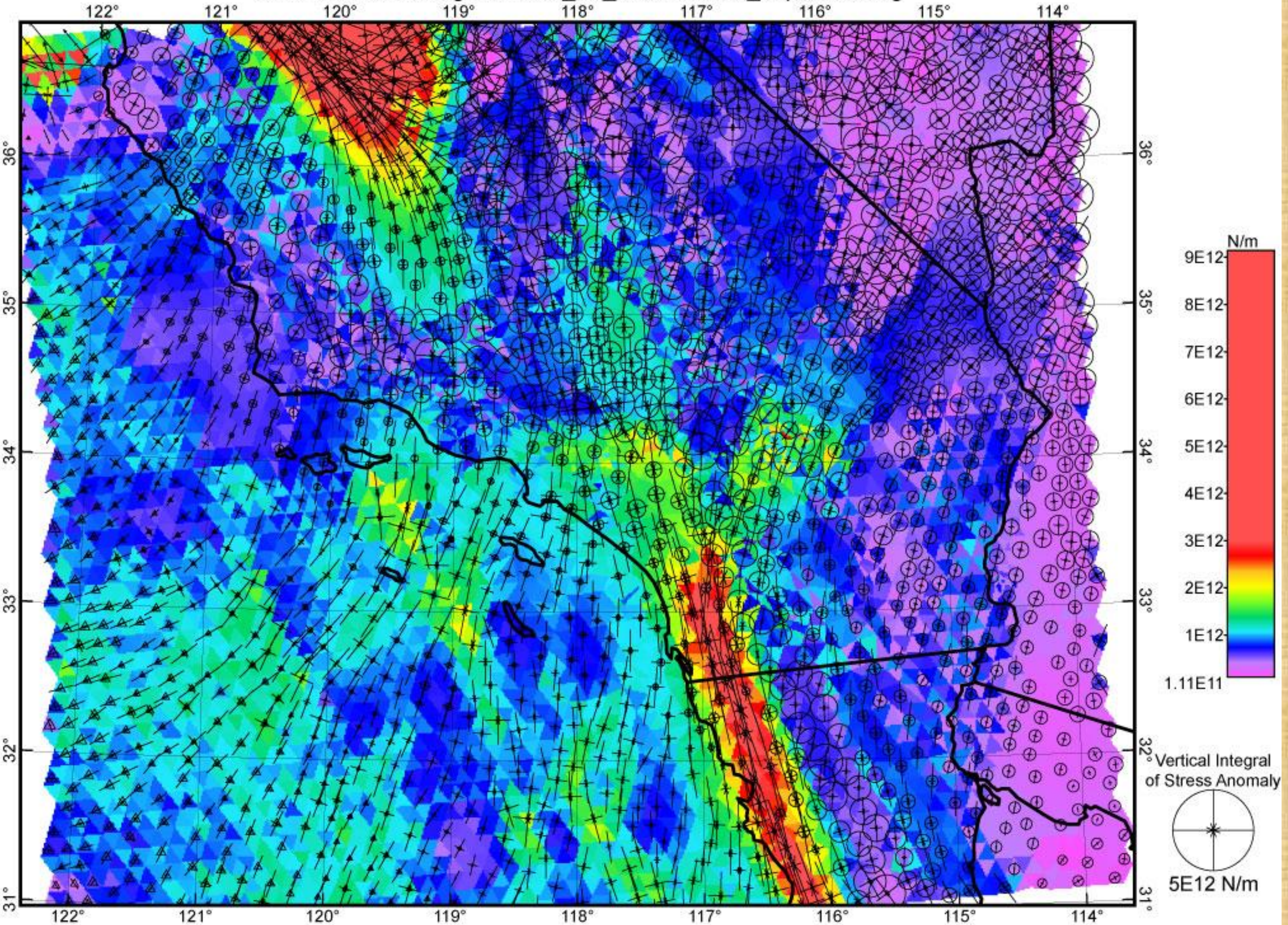

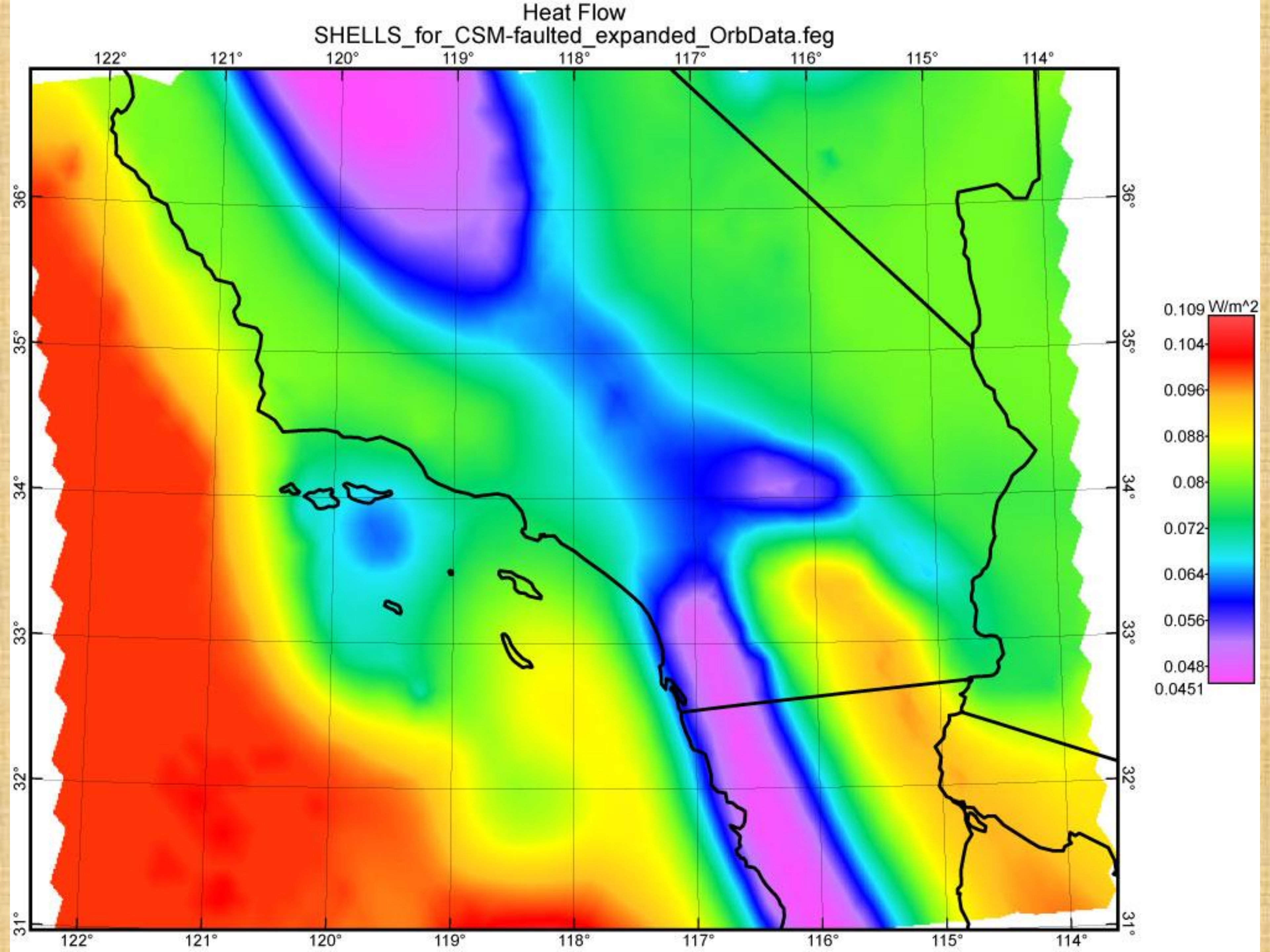
Heat Flow
SHELLS_for_CSM-faulted_expanded_OrbData.feg
122°
121°
120°
119°
118°
117°
116°
115°
114°
36°
35°
34°
33°
32°
31°
W/m^2
0.109
0.104
0.096
0.088
0.08
0.072
0.064
0.056
0.048
0.0451

Crustal Thickness
SHELLS_for_CSM-faulted_expanded_OrbData.feg

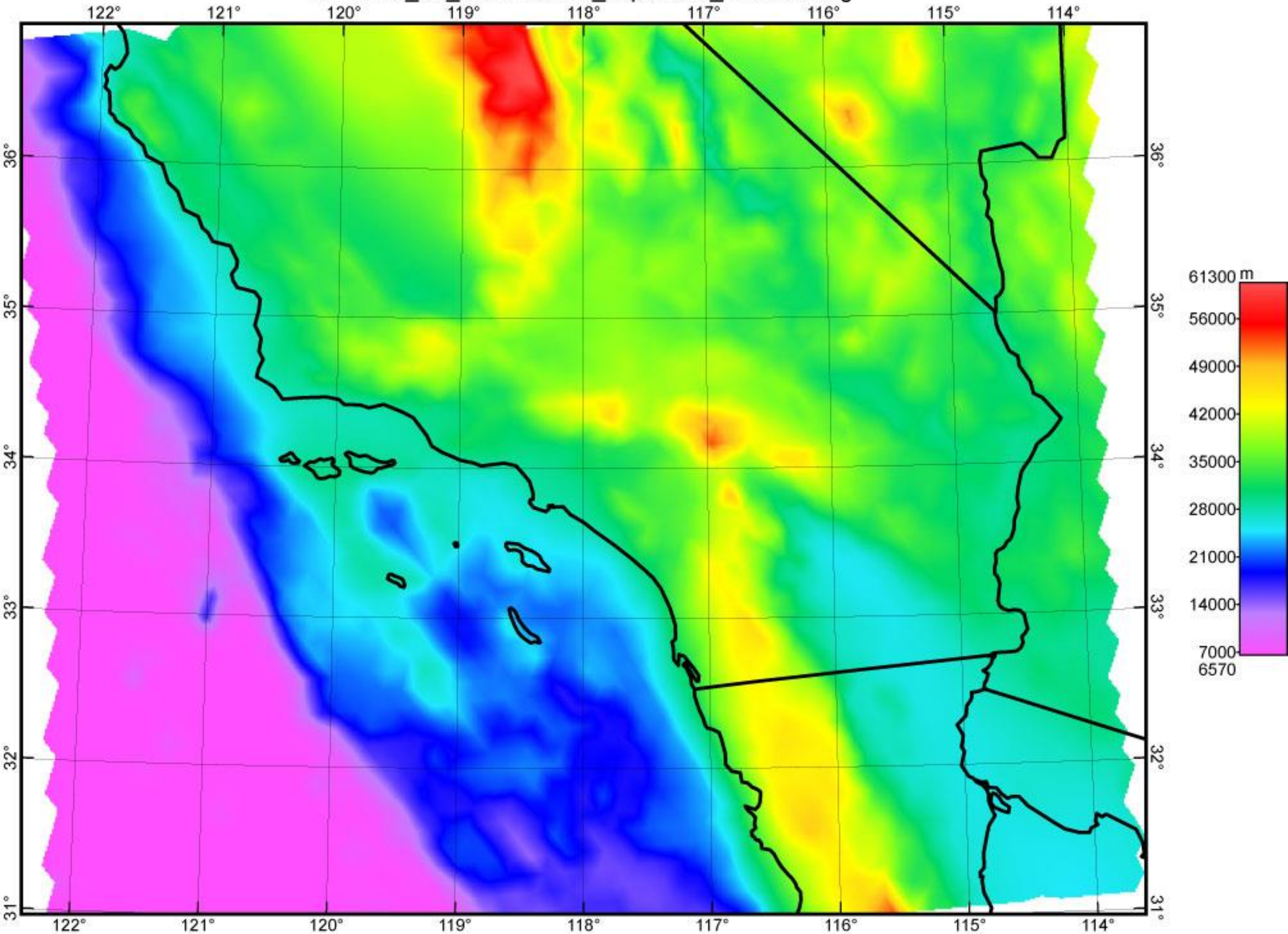

Total Lithosphere Thickness
SHELLS_for_CSM-faulted_expanded_OrbData.feg

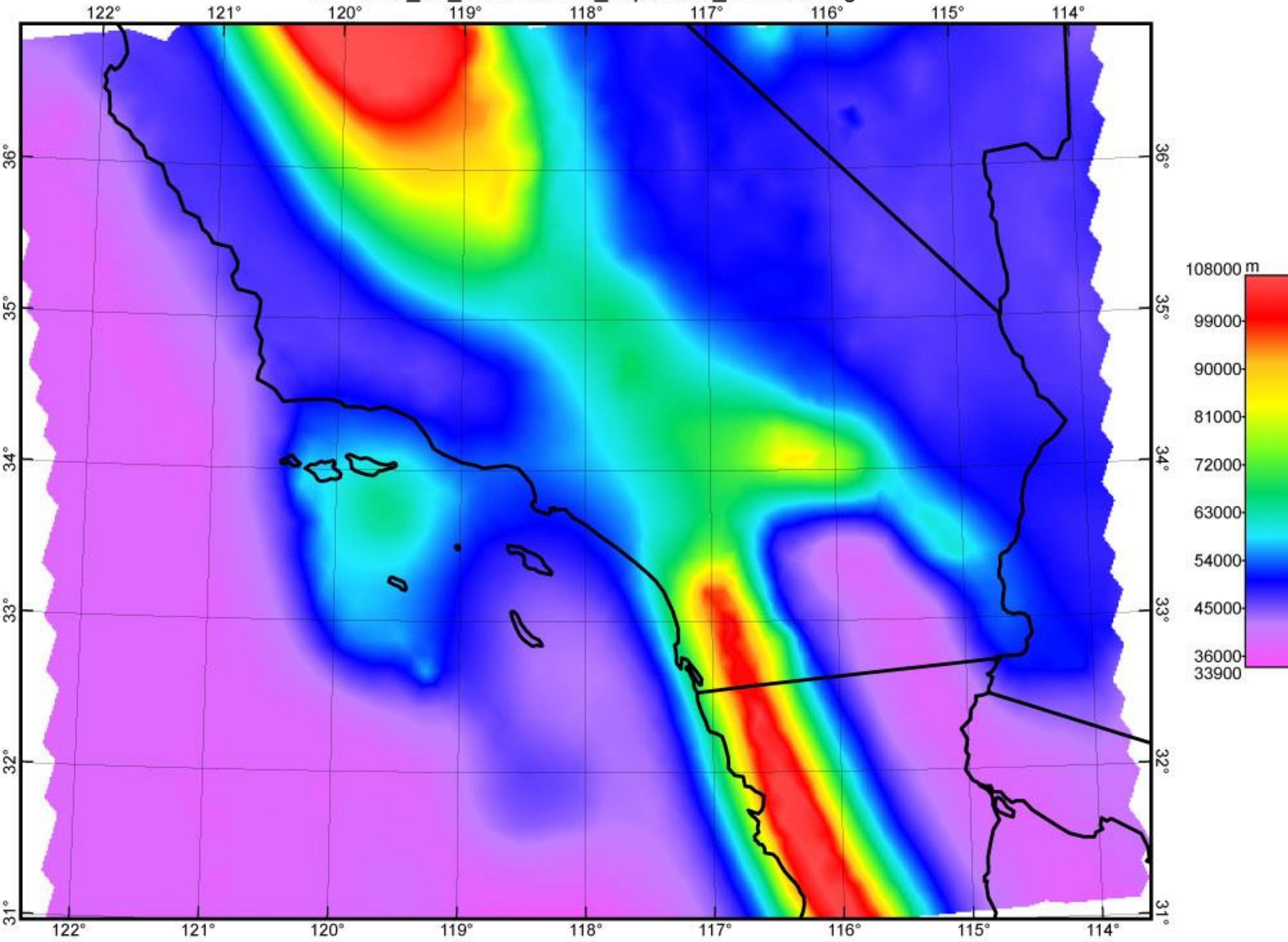

Change in Horizontal Velocity Across Faults
CSM2013001, using SHELLS_for_CSM-faulted_expanded.feg

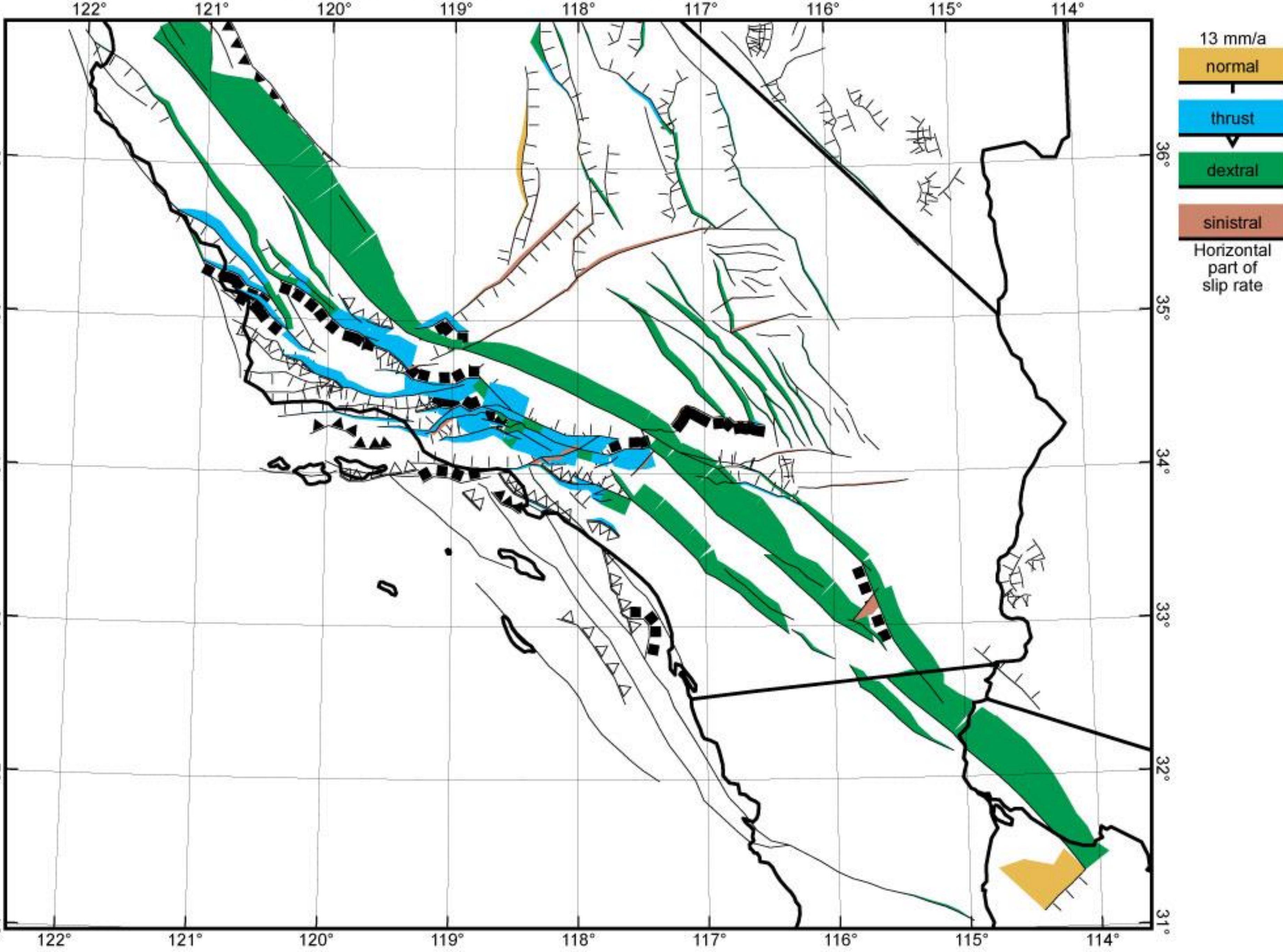

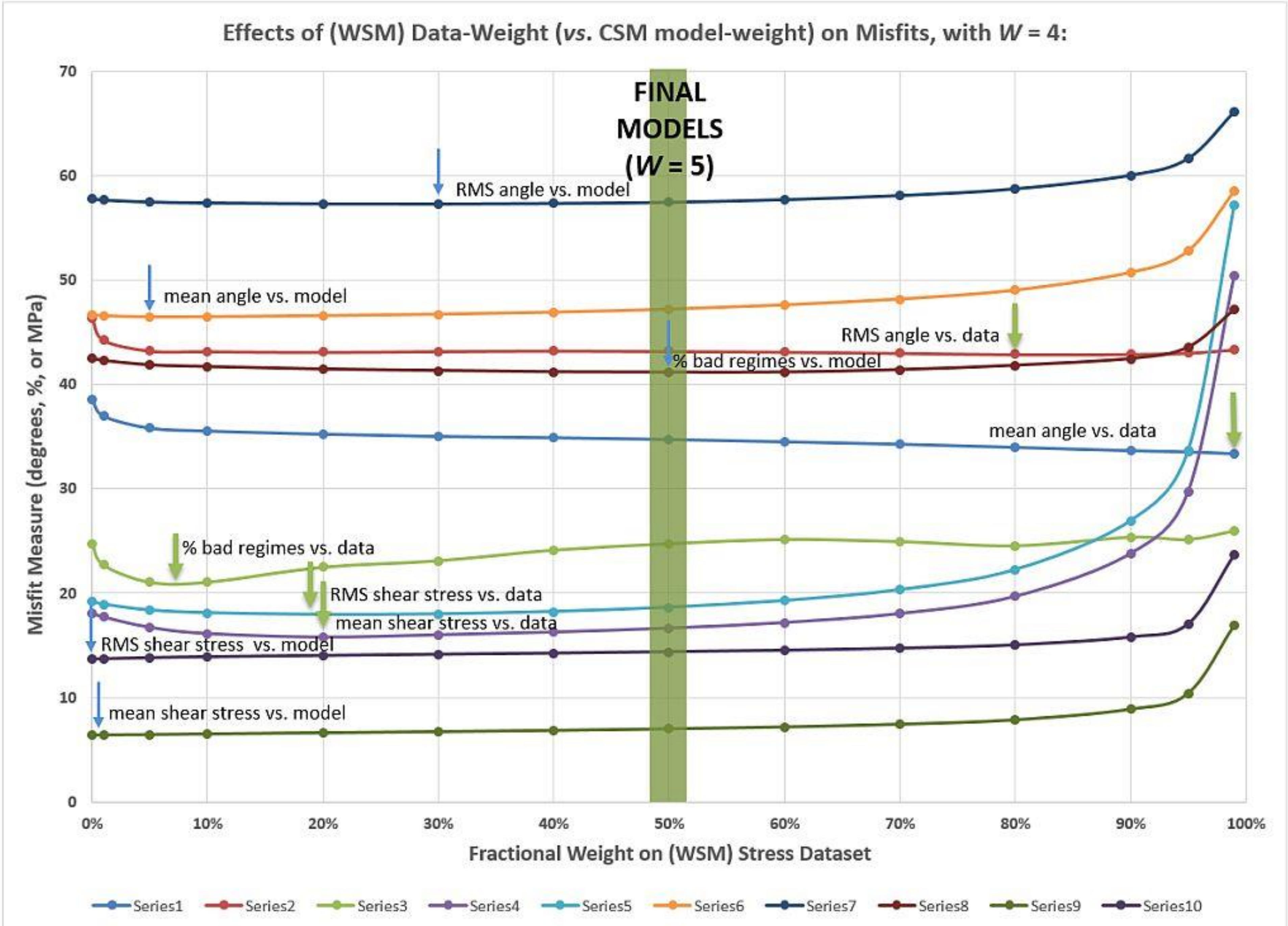
Effects of (WSM) Data-Weight (vs. CSM model-weight) on Misfits, with W = 4:
FINAL MODELS (W = 5)
RMS angle vs. model
mean angle vs. model
RMS angle vs. data
% bad regimes vs. model
mean angle vs. data
% bad regimes vs. data
RMS shear stress vs. data
mean shear stress vs. data
RMS shear stress vs. model
mean shear stress vs. model
Misfit Measure (degrees, %, or MPa)
70
60
50
40
30
20
10
0
0%
10%
20%
30%
40%
50%
60%
70%
80%
90%
100%
Fractional Weight on (WSM) Stress Dataset
Series1
Series2
Series3
Series4
Series5
Series6
Series7
Series8
Series9
Series10

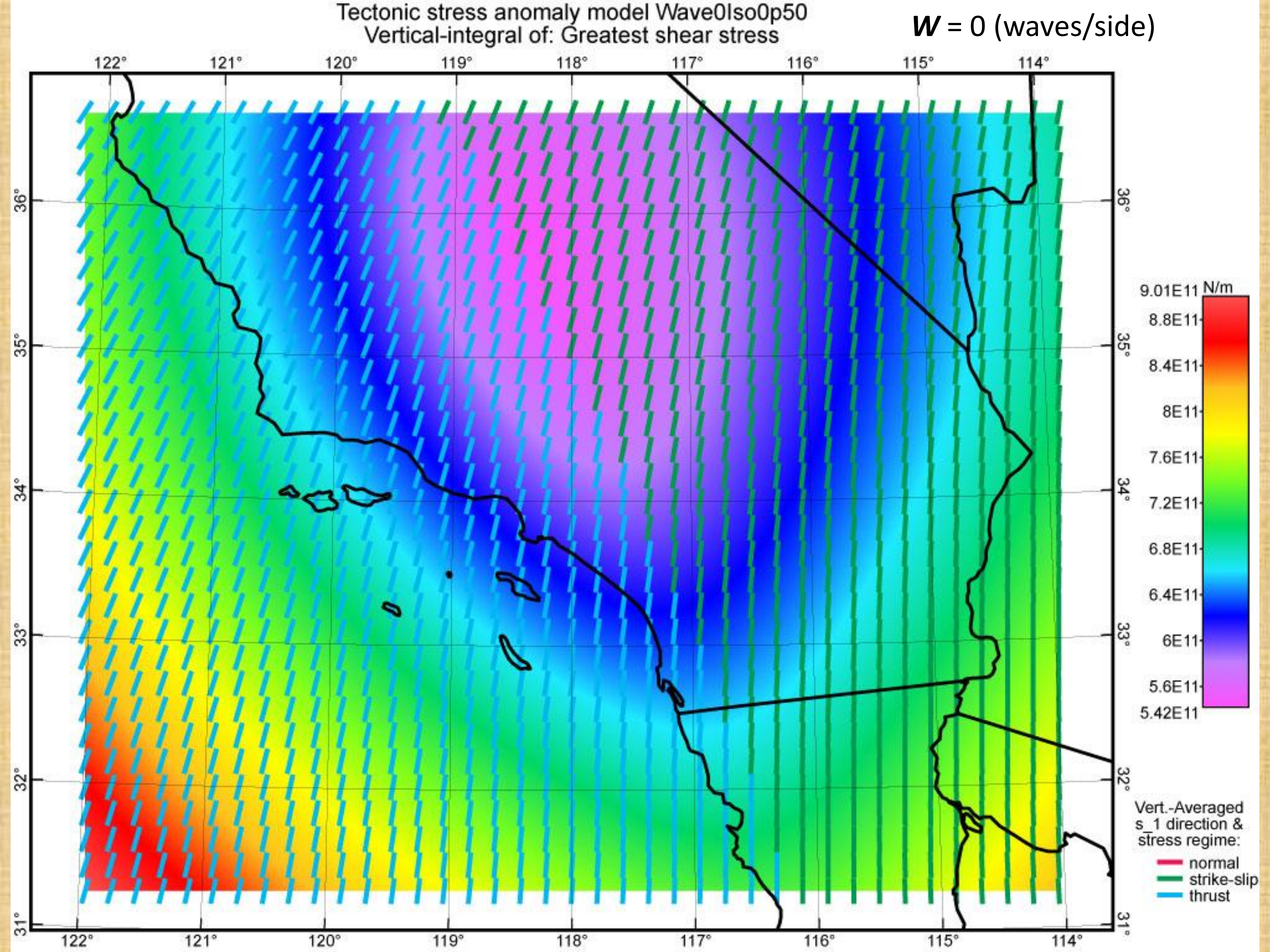
Tectonic stress anomaly model Wave0Iso0p50
Vertical-integral of: Greatest shear stress
W = 0 (waves/side)
122°
121°
120°
119°
118°
117°
116°
115°
114°
36°
35°
34°
33°
32°
31°
9.01E11 N/m
8.8E11
8.4E11
8E11
7.6E11
7.2E11
6.8E11
6.4E11
6E11
5.6E11
5.42E11
Vert.-Averaged
s_1 direction &
stress regime:
normal
strike-slip
thrust

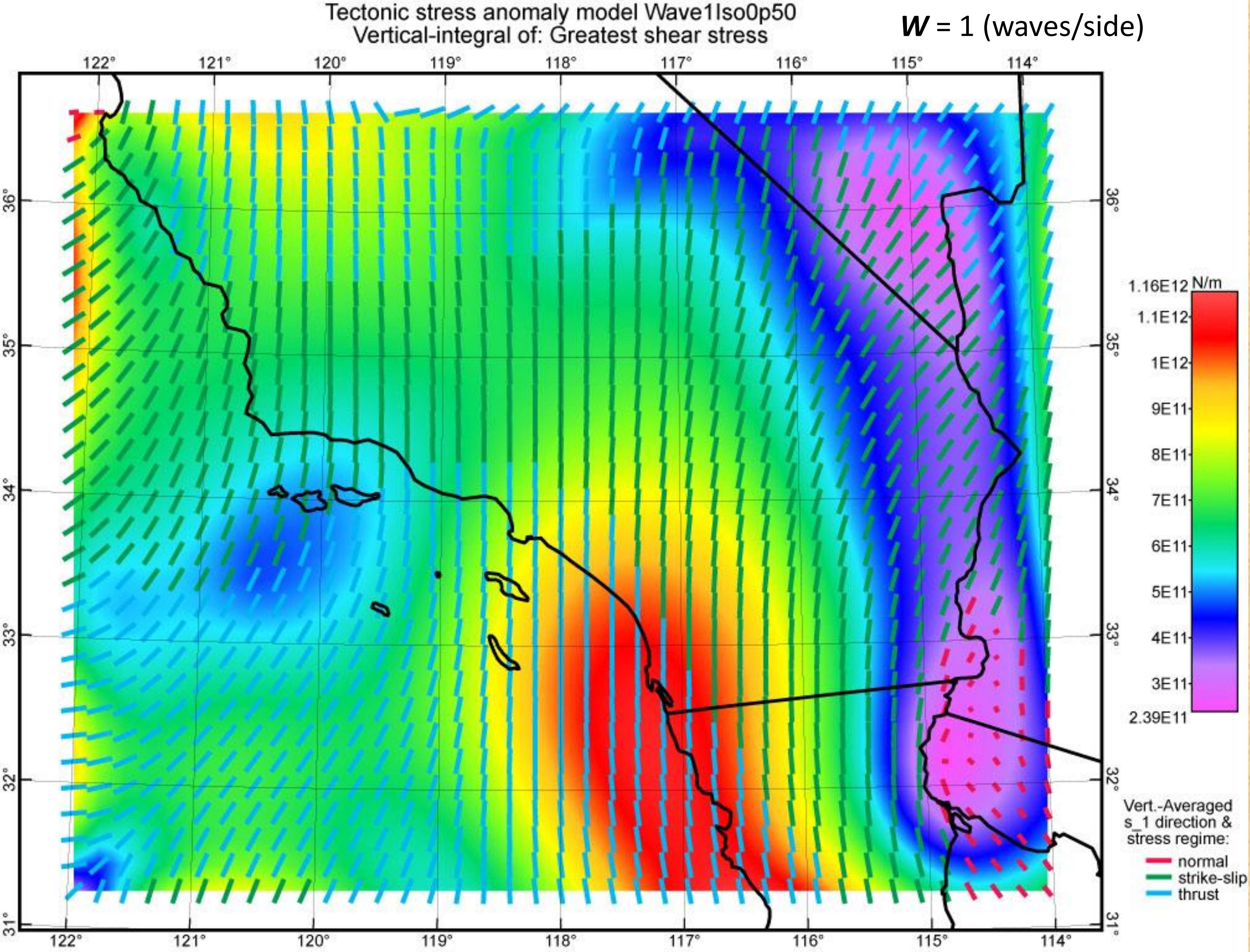
Tectonic stress anomaly model Wave1Iso0p50
Vertical-integral of: Greatest shear stress
W = 1 (waves/side)
122° 121° 120° 119° 118° 117° 116° 115° 114°
36° 35° 34° 33° 32° 31°
1.16E12 N/m
1.1E12
1E12
9E11
8E11
7E11
6E11
5E11
4E11
3E11
2.39E11
Vert.-Averaged s_1 direction & stress regime:
normal
strike-slip
thrust

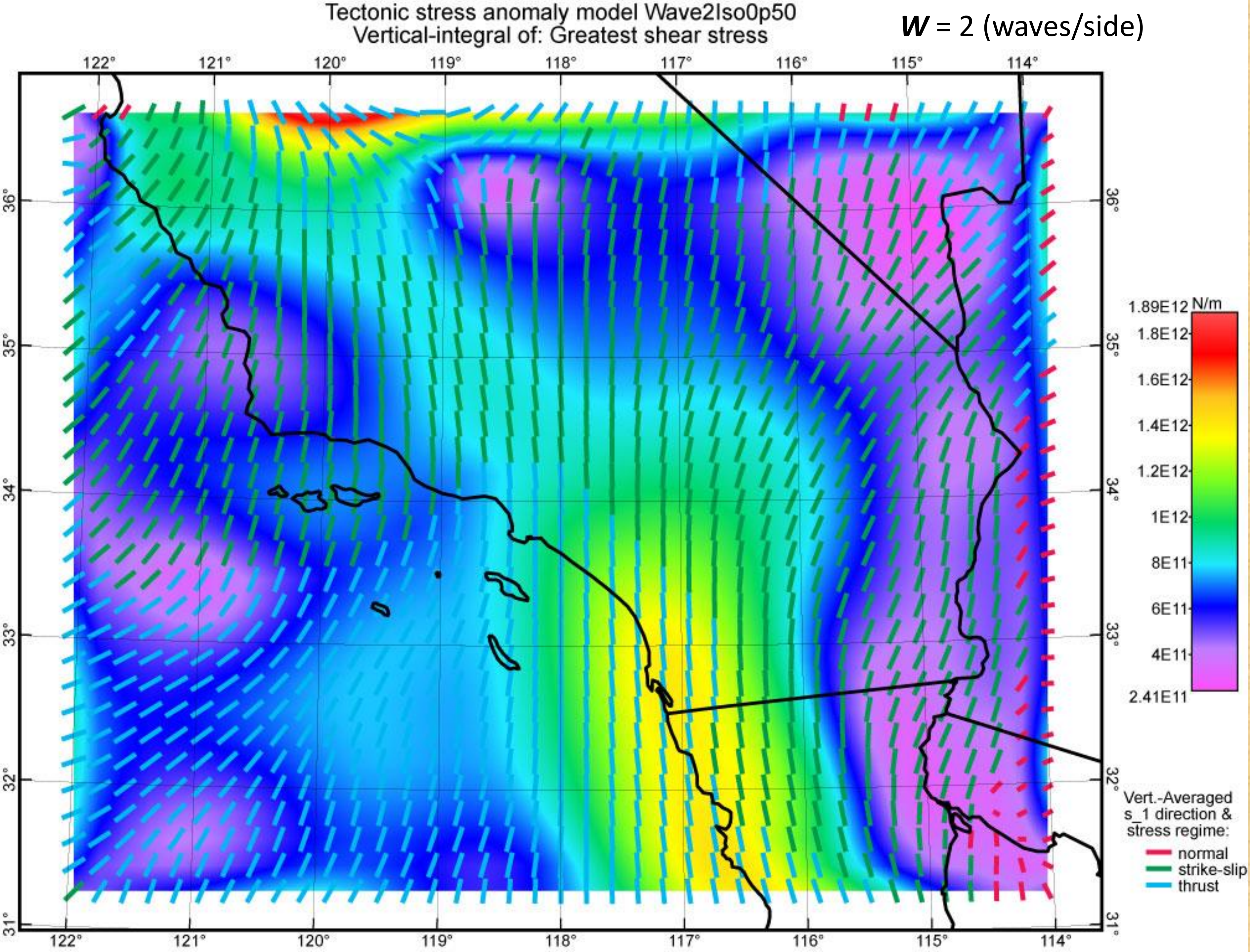

Tectonic stress anomaly model Wave2Iso0p50
Vertical-integral of: Greatest shear stress
W = 2 (waves/side)
122°
121°
120°
119°
118°
117°
116°
115°
114°
36°
35°
34°
33°
32°
31°
1.89E12 N/m
1.8E12
1.6E12
1.4E12
1.2E12
1E12
8E11
6E11
4E11
2.41E11
Vert.-Averaged
s_1 direction &
stress regime:
normal
strike-slip
thrust

W = 3 (waves/side)

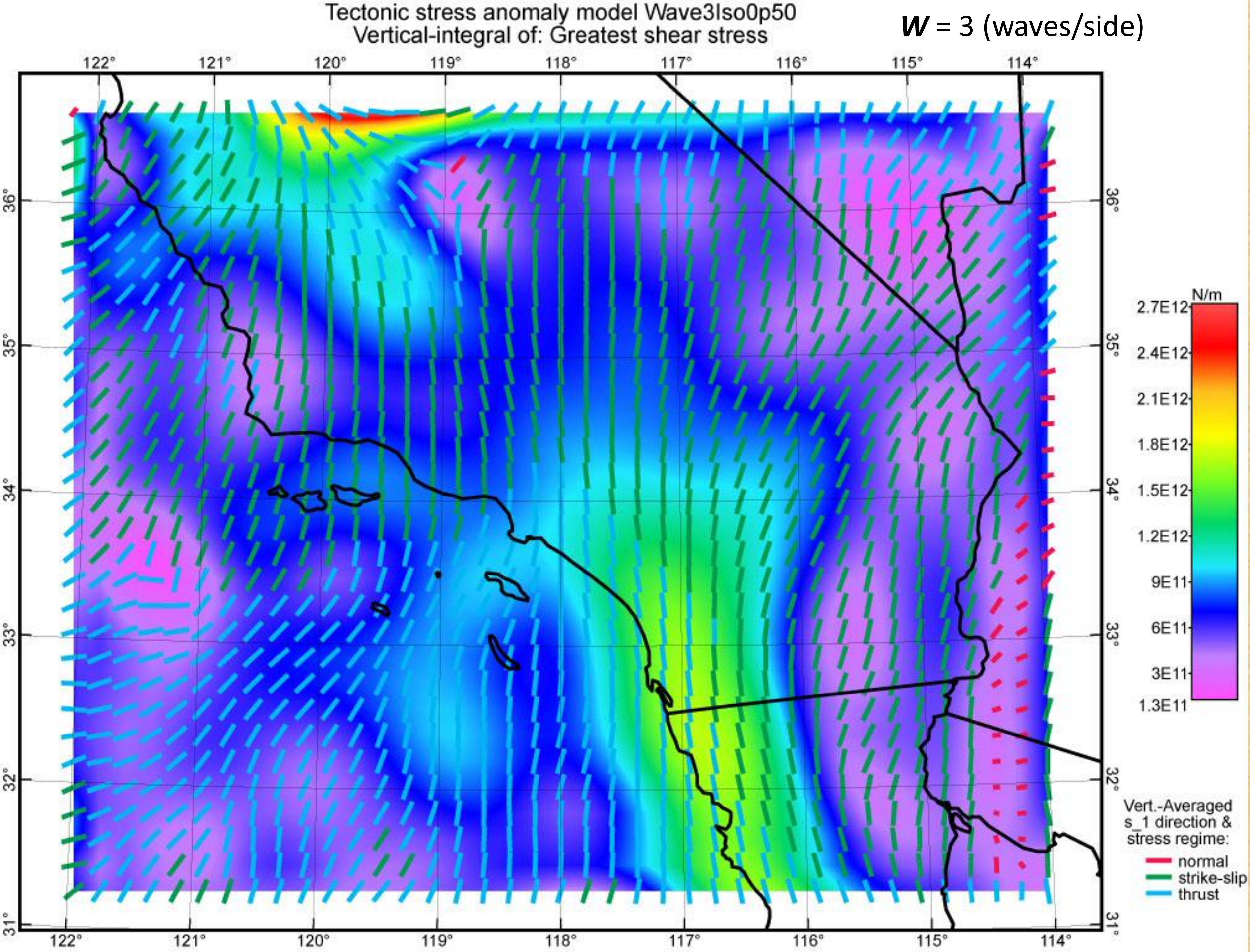

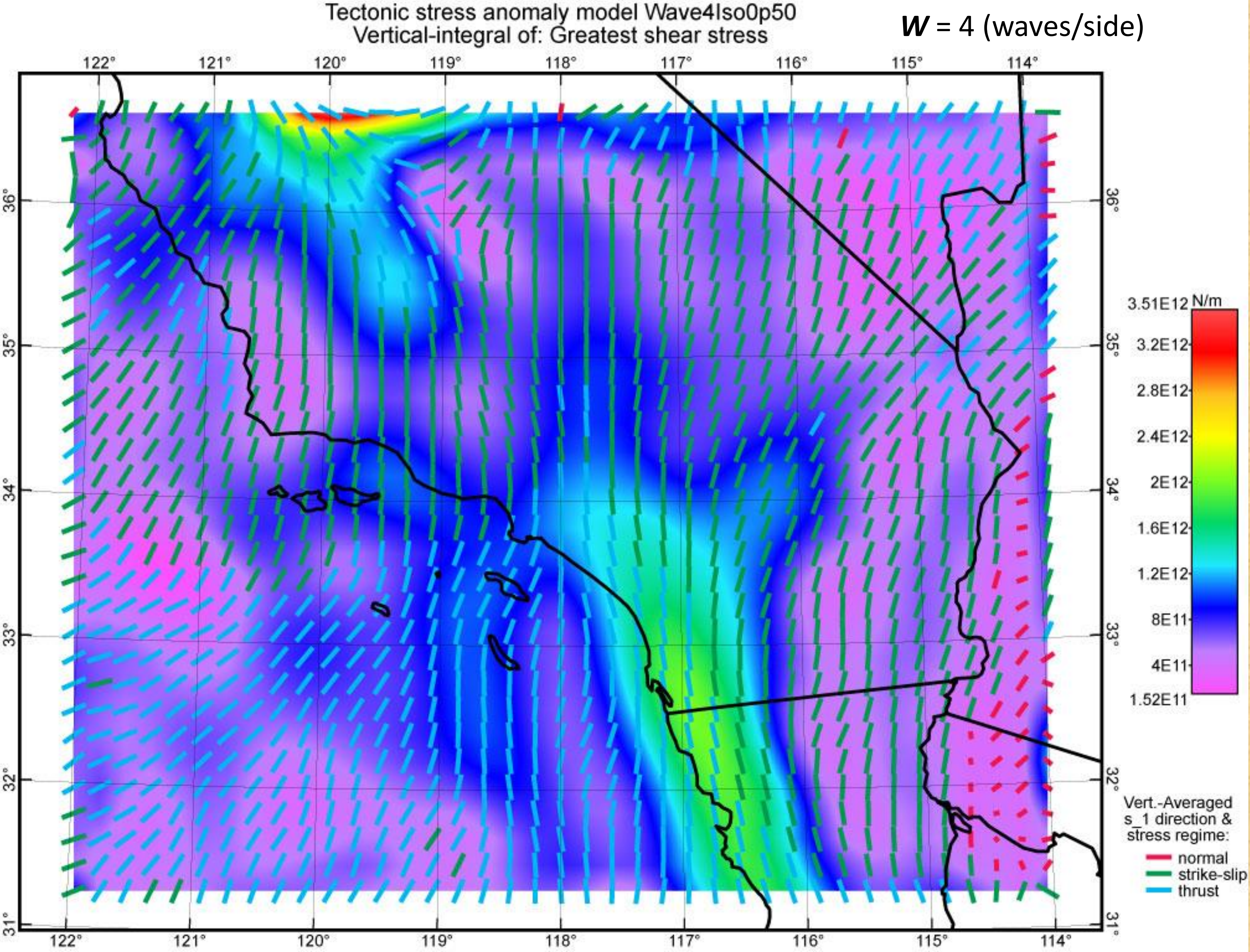
Tectonic stress anomaly model Wave4Iso0p50
Vertical-integral of: Greatest shear stress
W = 4 (waves/side)
122° 121° 120° 119° 118° 117° 116° 115° 114°
36° 35° 34° 33° 32° 31°
3.51E12 N/m
3.2E12
2.8E12
2.4E12
2E12
1.6E12
1.2E12
8E11
4E11
1.52E11
Vert.-Averaged s_1 direction & stress regime:
normal
strike-slip
thrust

W = 5 (waves/side)

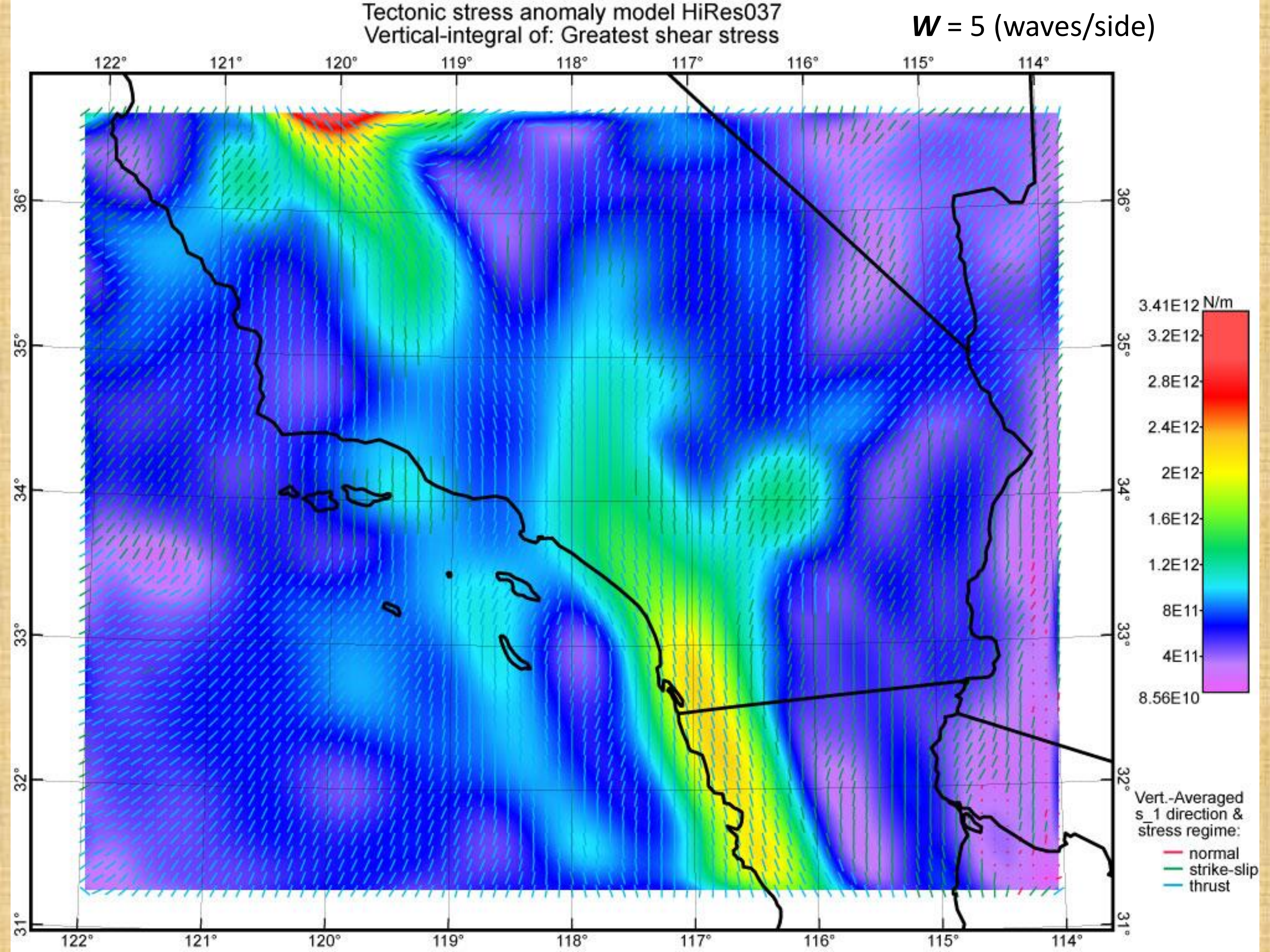

Total stress anomaly model HiRes037
Vertical-integral of: Greatest shear stress

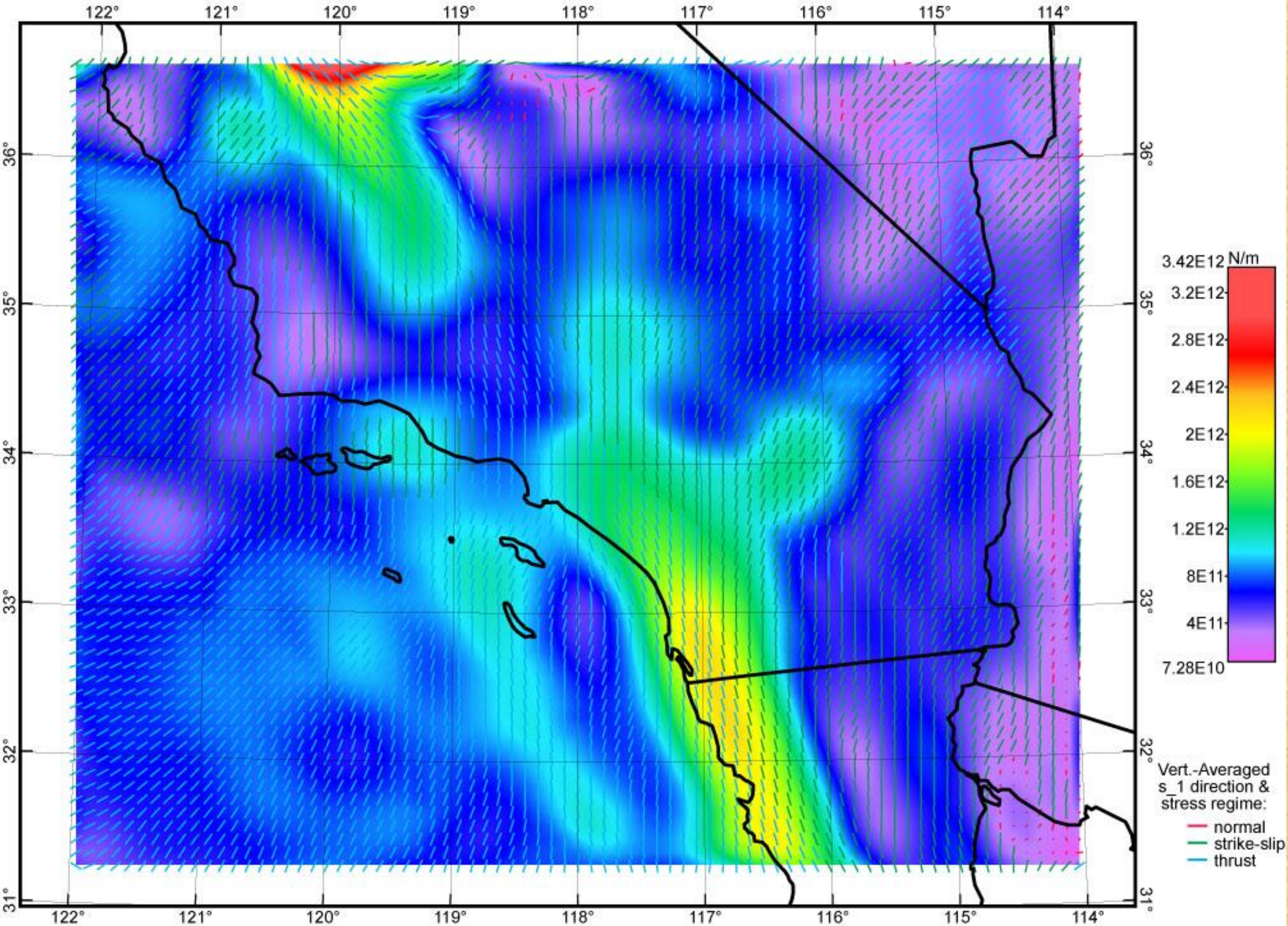

Total stress anomaly model HiRes037
Vertical-integral of: Greatest shear stress

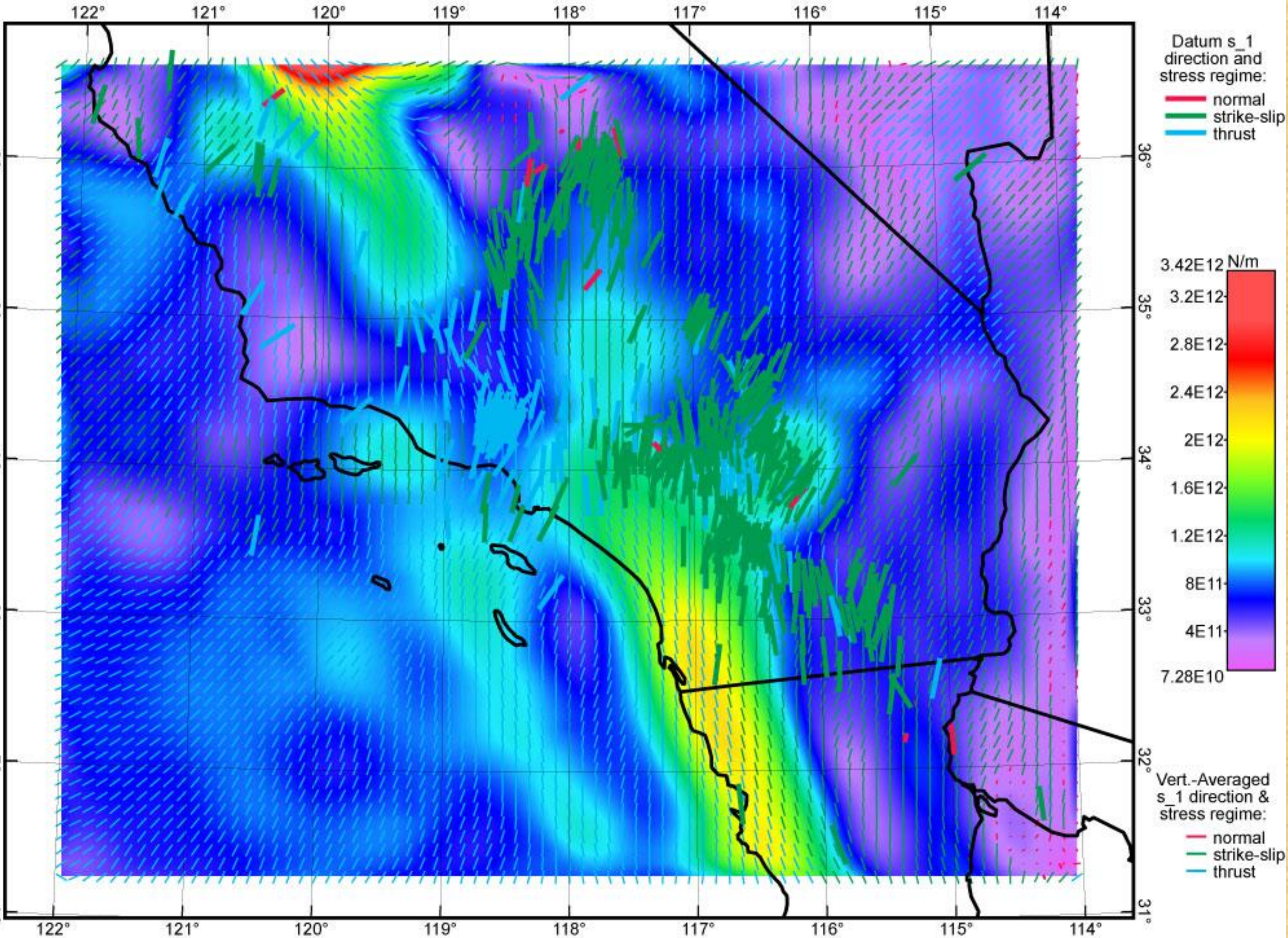

Total stress anomaly model HiRes037
Greatest shear stress in horizontal plane 10 km below MSL

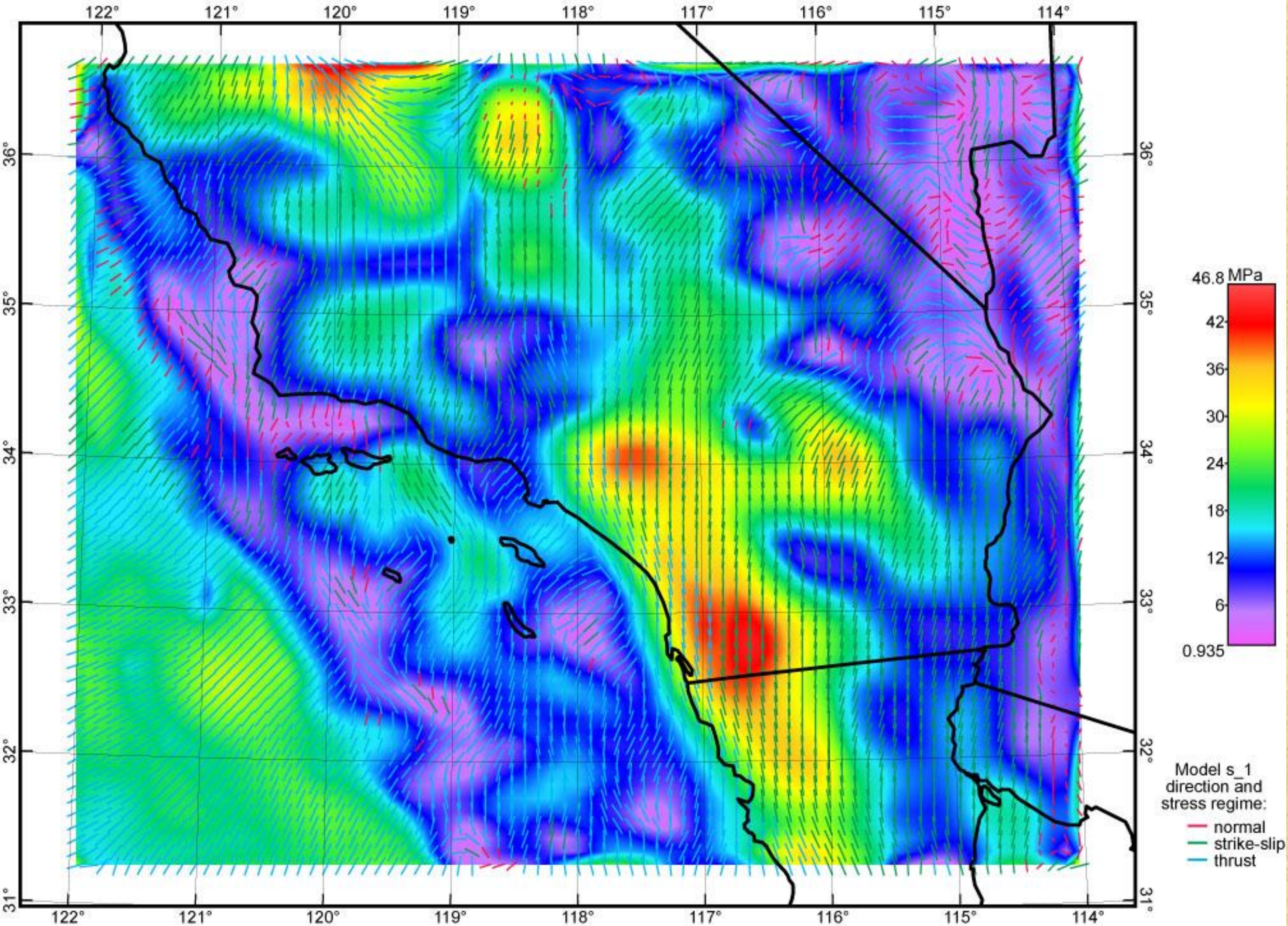

Total stress anomaly model HiRes037
Greatest shear stress in horizontal plane 10 km below MSL

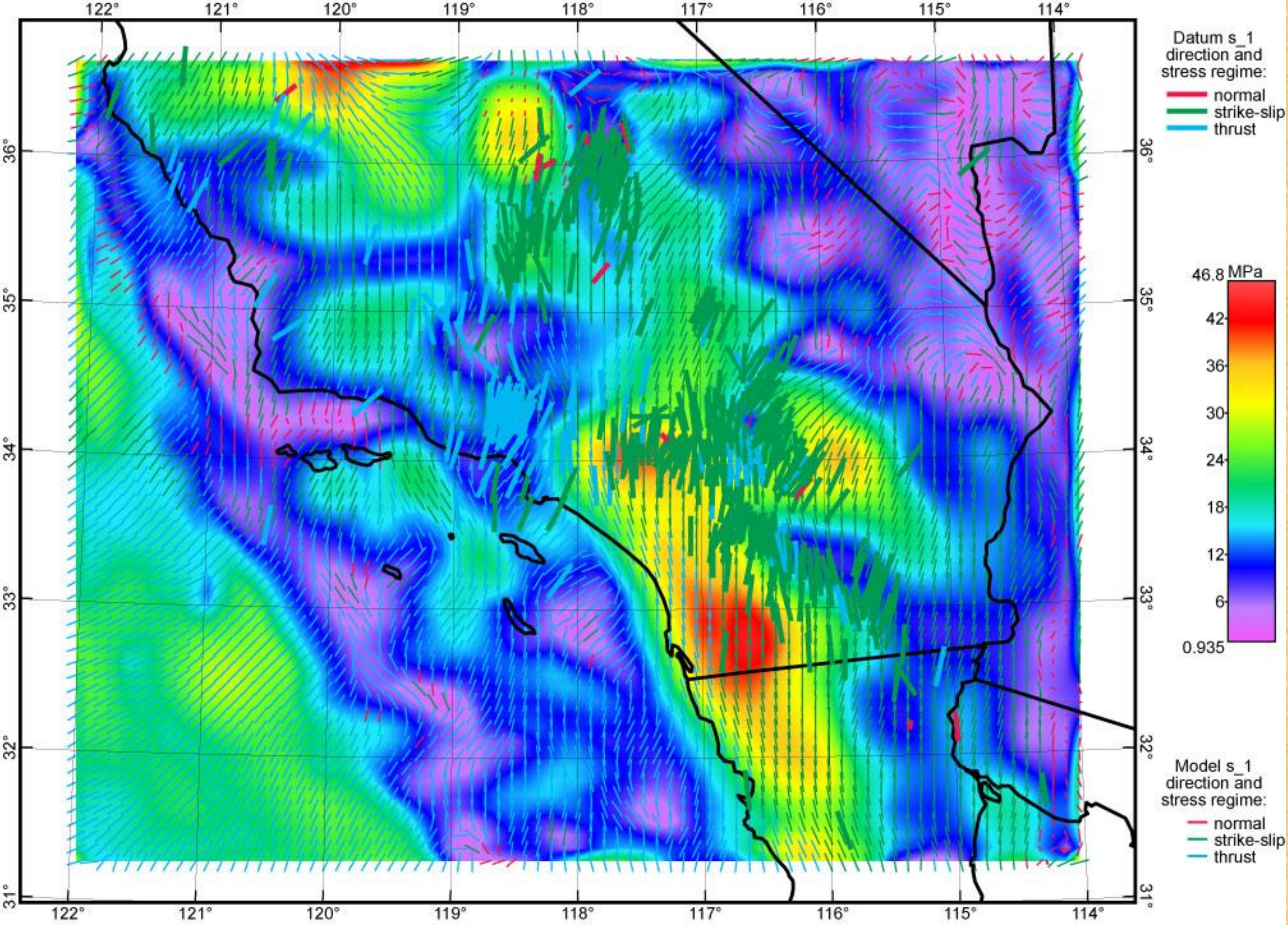

Total stress anomaly model HiRes037
Pressure anomaly at plane of section

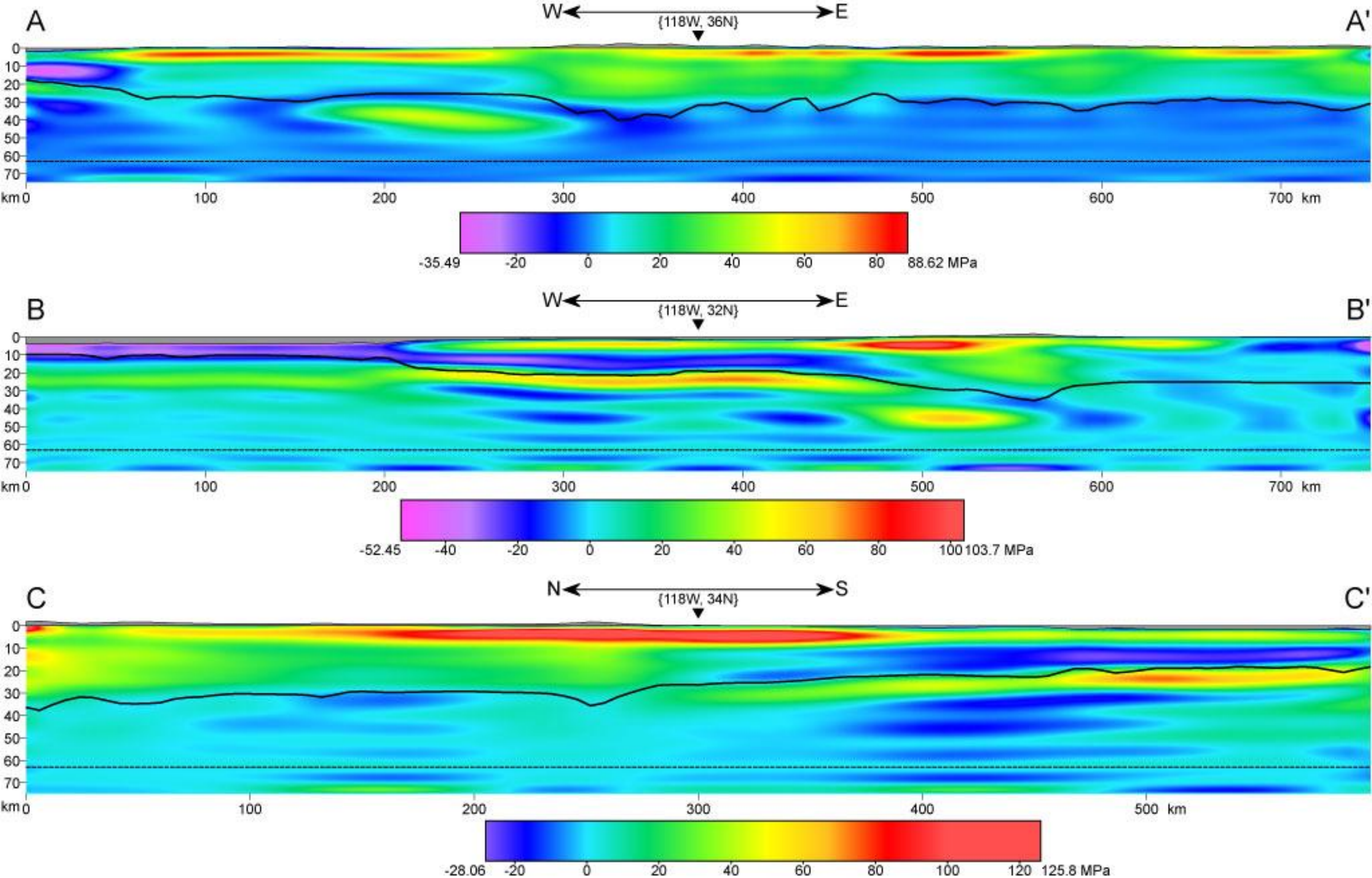

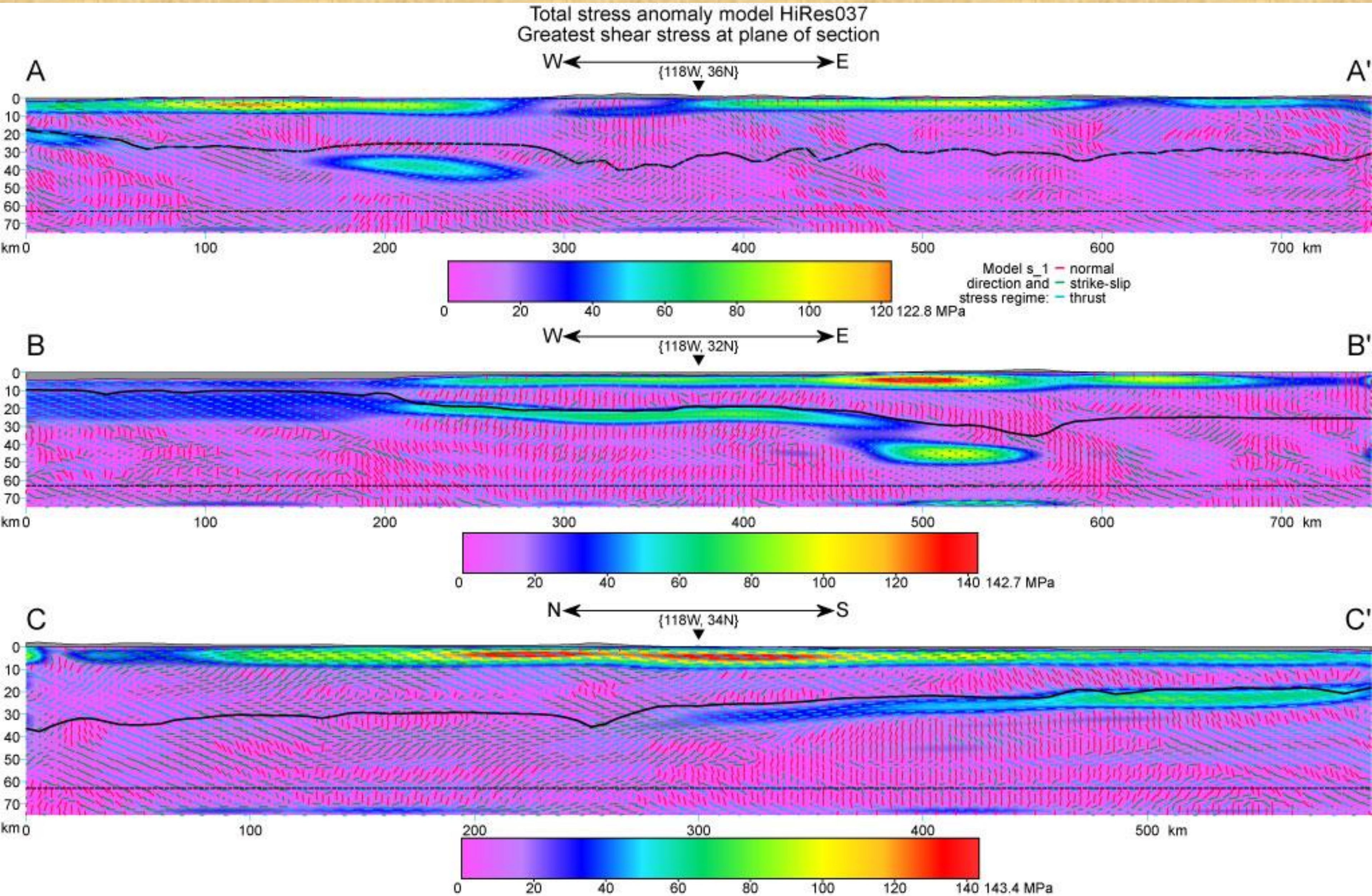
Total stress anomaly model HiRes037
Greatest shear stress at plane of section
A
A'
W
E
{118W, 36N}
km
0 10 20 30 40 50 60 70
0 100 200 300 400 500 600 700 km
0 20 40 60 80 100 120 122.8 MPa
Model s_1 direction and stress regime:
normal
strike-slip
thrust
B
B'
{118W, 32N}
0 20 40 60 80 100 120 140 142.7 MPa
C
C'
N
S
{118W, 34N}
0 100 200 300 400 500 km
0 20 40 60 80 100 120 140 143.4 MPa

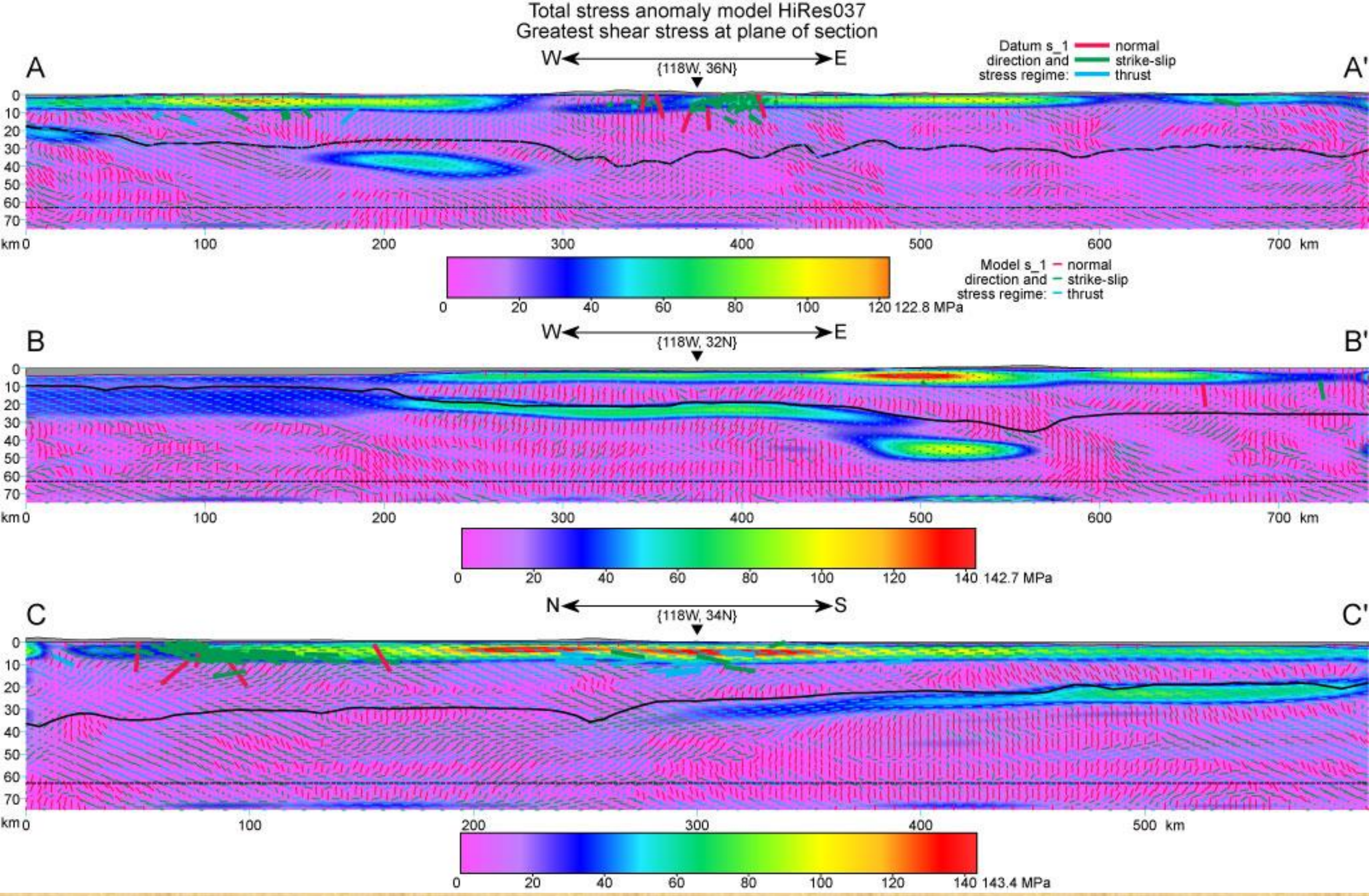
Total stress anomaly model HiRes037
Greatest shear stress at plane of section
A
W
E
{118W, 36N}
Datum s_1 direction and stress regime:
normal
strike-slip
thrust
A'
0
10
20
30
40
50
60
70
km 0
100
200
300
400
500
600
700 km
0
20
40
60
80
100
120 122.8 MPa
Model s_1 direction and stress regime:
normal
strike-slip
thrust
B
W
E
{118W, 32N}
B'
0
10
20
30
40
50
60
70
km 0
100
200
300
400
500
600
700 km
0
20
40
60
80
100
120
140 142.7 MPa
C
N
S
{118W, 34N}
C'
0
10
20
30
40
50
60
70
km 0
100
200
300
400
500 km
0
20
40
60
80
100
120
140 143.4 MPa

The **FlatMaxwell** algorithm and program represent important advances in stress modeling, in 3 ways:

1. It is now possible to ***merge stress data*** (which are usually just stress directions, and come primarily from the upper crust) ***with output from dynamic models*** (based on laboratory flow laws, plate-velocity boundary conditions, and computed geotherms) which constrain the likely magnitudes of deviatoric stresses and also the likely form of the mantle stress field.

2. **FlatMaxwell** is ***free of assumptions about*** *which* ***flow laws*** (and flow-law constants) regulate the level of deviatoric stress. Admittedly, such assumptions are made in program **Shells**, which contributed an important input dataset to this modeling effort. However, replacing this **Shells** dataset with that from a competing dynamic model would be relatively easy, and would not require any reprogramming.

3. Stress fields in **FlatMaxwell** ***obey the quasi-static equilibrium equation exactly***, at all points. This is superior to stress fields obtained from finite-element models which solve a weak form of equilibrium (sometimes weakened further by vertical integration) on a coarse grid.